Transportation Research Part B 159 (2022) 24–48

Contents lists available at ScienceDirect

Transportation Research Part B

journal homepage: www.elsevier.com/locate/trb

Review

Optimization model for the freeway-exiting position decision problem of automated vehicles

Da Yang [a,b], Bingmei Jia [a], Liyuan Dai [a], Jing Peter Jin [c], Lihua Xu [d,*], Fei Chen [e], Shiyu Zheng [a], Bin Ran [b]

[a] School of Transportation and Logistics, National Engineering Laboratory of Integrated Transportation Big Data Application Technology, National United Engineering Laboratory of Integrated and Intelligent Transportation, Southwest Jiaotong University, Chengdu, 611756, China
[b] Department of Civil and Environmental Engineering, University of Wisconsin-Madison, Madison, 53706, USA
[c] Department of Civil and Environmental Engineering, Rutgers, The State University of New Jersey, Piscataway, NJ 08854, USA
[d] School of Physical Science and Technology, Southwest Jiaotong University, Chengdu, 611756, China
[e] Sichuan Intelligent Highway Technology Co., Ltd., Chengdu, 610041, China

A R T I C L E I N F O

Keywords:
Automated vehicles
Lane change
Freeway-exiting position decision
Exiting success probability
Optimal exiting decision point

A B S T R A C T

In recent years, automated vehicles have attracted much attention all over the world. This paper focuses on the freeway-exiting position decision problem of automated vehicles (AVs). Specifically, the paper addresses the determination of the lane-changing initiation location in the process of exiting the freeway. The location of the freeway-exiting decision point has a significant impact on the safety and efficiency of automated vehicles. If the lane-changing location is too close to the off-ramp, the AV may not succeed in exiting and may even collide with other vehicles. If the decision point is too far from the off-ramp, the AV will enter into the slower lane too early, increasing the travel time. However, the freeway-exiting lane-changing position problem of AVs has not been investigated thoroughly in the existing literature. This paper proposes a freeway-exiting position decision model to find the optimal freeway-exiting decision position to balance the efficiency and safety in the freeway-existing process. Field data is collected to validate the proposed model, and simulations are also conducted to analyze the variations of the exiting success probability (ESP) and the optimal exiting decision (OED) position under various traffic conditions. The results show that the proposed model can predict the value of ESP with high performance (MAPE is less than 13%) and help an automated vehicle to generate an appropriate freeway-exiting decision point to ensure a high ESP without sacrificing efficiency. An AV can increase its ESP by decreasing or increasing its speed to meet more safe lane-changing gaps on the target lane, and the speed-decreasing method has a more significant effect than the speed-increasing method. The speed difference between the two adjacent lanes greatly influences ESP and the OED point, and maintaining the speed difference in an appropriate range can increase ESP.

1. Introduction

In recent years, autonomous driving has become a hot topic and attracts worldwide attention (Zhou et al., 2020/02/01, Luo et al.,

* Correspondence author.
E-mail address: xulihua@swjtu.edu.cn (L. Xu).

https://doi.org/10.1016/j.trb.2022.03.003
Received 23 May 2021; Received in revised form 28 February 2022; Accepted 15 March 2022
Available online 21 March 2022

2019/11/01, Yu et al., 2019). Automated vehicles (AVs) are considered to have a huge potential to enhance traffic safety (Ma et al., 2017), ease traffic congestion (Sun, Zheng and Sun, 2020), improve traffic flow stability (Zhou and Ahn, 2019), and reduce traffic pollution (Li and Li, 2019). AVs have now been intensively tested on real-world roadway networks, such as Waymo (Nourinejad, Bahrami and Roorda, 2018), (Mobileye et al., 2020), and nuTonomy (Mattioli, 2018, Cui et al., 2018), and the industry and research community believe that AVs may develop rapidly in the future decades (Berger and Rumpe, 2014, Shladover, 2018).

This paper focuses on a critical decision problem of AVs, called the freeway-exiting position decision problem. The freeway-exiting position decision refers to that an AV decides where to leave the freeway by the closest off-ramp. When the AV arrives at the freeway-exiting position decision point, the AV will start to move to the outmost lane from the current lane. Since the freeway-exiting decision position is the starting point of the freeway-exiting process of AVs, it has a significant impact on the subsequent freeway-exiting trajectory Fig. 1. illustrates an example of the freeway-exiting process of an AV. In the figure, the AV locates on the leftmost lane (Lane 3) at first and intends to leave the freeway by the off-ramp. To reach the off-ramp, the AV needs to change to Lane 2 first and then change to Lane 1. The dashed red lines in Fig. 1 represent the freeway-exiting trajectories corresponding to the two different freeway-exiting decision points A and B, and point B is much closer to the off-ramp than point A. Starting the freeway-exiting process from point A needs to consume more time than point B, because in this case, the AV will enter into the slower lanes earlier. However, starting the exiting process from point B will decrease the success probability of exiting the freeway because the time left for the two lane-changings from Lane 3 to Lane 1 is much shorter. Especially when the chosen freeway-exiting decision point is too close to the off-ramp, the AV may not be able to succeed to exit the freeway by the off-ramp or crash with the vehicles on Lane 1 if it tries to force a lane-changing. Therefore, the freeway-exiting decision point has a significant impact on the efficiency and safety of AVs in the freeway-exiting process, and choosing an appropriate decision point is critical to AVs. However, finding an optimal exiting lane-changing location is a complex problem, especially when an automated vehicle has multiple lanes to cross to reach the off-ramp.

This paper investigates the freeway-exiting position decision problem to determine the appropriate freeway-exiting decision position for AVs that can ensure a high successful freeway-exiting probability without sacrificing too much travel time in the freeway-exiting process. In the existing studies (Ardelt, Coester and Kaempchen, 2012, Ali et al., 2019, Tarko, Shamo and Wasson, 1999, Saad et al., 2018), two areas are related to the freeway-exiting position decision problem. The first one is the mandatory lane-changing decision of AVs, which tries to decide whether the target lane is safe for a lane-changing, when/where to execute a lane-changing, and the gap on the target lane can be accepted, which is part of the freeway-exiting position decision problem. The second one is the lane-changing advisory for human drivers in the weaving segment on freeways, aiming to reduce traffic delay by suggesting a lane-changing position to drivers, which aims to control all vehicles to improve traffic efficiency but not make a lane-changing decision for an individual vehicle. Although the two topics are similar to the problems in this paper, they have significant differences, and the proposed methods in the existing studies cannot be applied to solve the freeway-exiting decision position problem of AVs. This paper explores the relationship between the exiting success probability (ESP) and the freeway-exiting decision position and developed an optimal exiting decision (OED) model to ensure safety and efficiency. Field data were collected to validate the proposed model, and numerical simulations were used to analyze the critical impact factors, such as the average speed of traffic flow, the speed difference between adjacent lanes, etc., on ESP and the OED point.

The rest of the paper is organized as follows Section 2. reviews the existing studies relevant to the freeway-exiting position decision problem Section 3. proposes the ESP models for both the two-lane and multi-lane scenarios, and then an optimal exiting decision model is proposed Section 4. is model calibration and validation Section 5. explores the characteristics of the proposed model by simulations, and Section 6 concludes this paper and discusses the future work.

2. Literature review

In this section, three topics of literature related to this study are reviewed. The first topic is on the mandatory lane-changing decision of AVs since the freeway-exiting maneuver is a type of mandatory lane-changing. The second topic is the lane-changing advisory for human drivers in the merge segments of freeways. The third topic is the lane-changing decision before an off-ramp for human drivers.

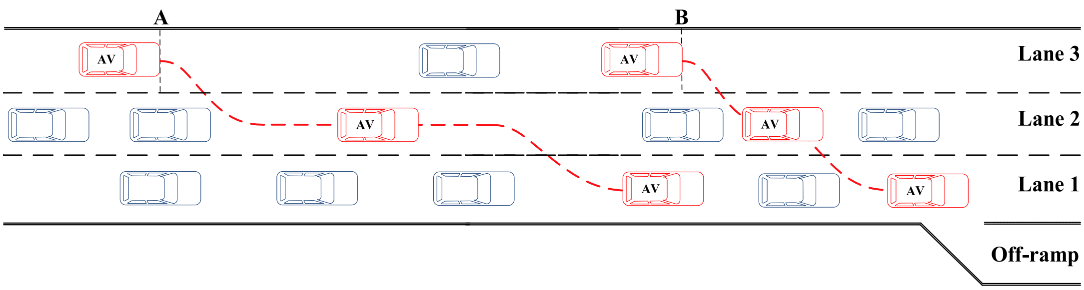

Fig. 1. Freeway-exiting position decision scenario of an automated vehicle on a freeway

2.1. Mandatory lane-changing decision of automated vehicles

The existing models of the mandatory lane-changing (MLC) decision of automated vehicles include rule-based models, utility-based models, and artificial intelligence models.

The rule-based models try to formulate the lane-changing decision by setting some rules for AVs. Ardelt et al. (Ardelt, Coester and Kaempchen, 2012) proposed a lane-changing decision model for AVs. Several rules were introduced to judge the necessity and feasibility of lane-changing considering the target place and the surrounding traffic conditions. Kumar et al. (Kumar et al., 2018) proposed a motion planning framework for the merging maneuver of AVs. The framework was a rule-based two-layer structure that could guarantee collision-free merging even in dense traffic. Hu and Sun (Hu and Sun, 2019) developed a set of control rules for a multi-lane freeway merging system. The cooperative lane-changing and merging were optimized separately and then combined to form a complete control system. Dong et al. (Dong et al., 2020) developed a five-step process for the mandatory lane-changing decision of AVs, including environment perception, safe gap computation, measured gap ranking, measured gap classification, and gap selection.

The main idea of the utility-based models is to choose from following or lane-changing for AVs by evaluating the driving gain of each choice. Ali et al. (Ali et al., 2019) proposed a game theory-based mandatory lane-changing decision model for AVs in the connected environment. The model was assessed using the data collected in a connected environment where drivers made decisions with the help of driving aids. Awal et al. (Awal, Murshed and Ali, 2015) proposed an efficient cooperative lane-changing decision algorithm for AVs to reduce the lane-changing bottlenecks and minimize on-ramp merging time on freeways. The lane-changing location was determined based on the comparison of the utility and risk of different lanes. Cao et al. (Cao et al., 2017) proposed an optimal mandatory lane-changing decision model with the objective function as the minimum travel time, which determined the optimal position to change lanes when the AV approached the intersection on urban arterials.

The artificial intelligence models use algorithms, such as neural networks, decision trees, and Bayesian classification, to model the lane-changing location selection for AVs by training the models using human lane-changing data, providing a human-like control model for AVs. Hou et al. (Hou, Edara and Sun, 2014) developed a lane-changing assistance system that could advise drivers to maintain safe gaps in mandatory lane-changing using Bayes classifier and decision tree methods. Hart et al. (Hart, Rychly and Knoll, 2019) proposed a stochastic policy-based reinforcement learning method to solve the merging problem of AVs, which was iteratively executed to generate a guiding reference lane-changing trajectory. Dou et al. (Dou et al., 2018) proposed a gated branch neural network for the lane-changing decision of AVs driving on on-ramps, and their results showed that the proposed algorithm outperformed other traditional binary classifiers and was more lightweight than AlexNet which is a widely used deep Convolutional Neural Networks (CNN) algorithm proposed by Krizhevsky et al. (Krizhevsky, Sutskever and Hinton, 2017).

2.2. Lane-changing advisory for human drivers

The studies on the lane-changing advisory models attempt to lead human drivers to change lanes at optimal positions on freeways. The existing models can be divided into two categories, rule-based models and data analysis-based models.

The rule-based models apply rules to construct a dynamic merging segment to guide drivers in the merging process. The Indiana Department of Transportation and Purdue University (Tarko, Shamo and Wasson, 1999) proposed a traffic control system (Indiana Lane Merge System) of merging advisory before a work zone for human drivers. In the system, a dynamic traffic sign of "DO NOT PASS" was set up before the work zone, whose position was modeled as a power function of the length of the congested portion. The system adopts a simple rule that the sign was activated when traffic density exceeds a certain threshold. The Indiana Department of Transportation (Datta et al., 2004) designed a merging traffic control system named DELMTCS (Dynamic Early Lane Merge Traffic Control System), which was similar to the Indiana Lane Merge System (Tarko, Shamo and Wasson, 1999). Park and Smith (Park and Smith, 2012) developed a lane-changing advisory algorithm to address merging conflicts in the merging segment of the on-ramp by adopting the IntelliDrive technology, which encouraged vehicles on the mainline to change lanes to create more space for the merging vehicles. Schakel and Arem (Schakel and Arem, 2014) presented an in-vehicle lane-changing advisory system. The lane-changing advisory based on a series of advice rules was provided, aiming for obtaining the optimal distribution of vehicles on different lanes to reduce travel time. Mai et al. (Mai, Jiang and Chung, 2016) developed some lane-changing advisory rules in a weaving segment based on C-ITS (Cooperative Intelligent Transport Systems). They divided all vehicles into four groups by assigning random numbers (each group has a different lane-changing area). The results indicated that the proposed rules could significantly reduce traffic delays. Zhang et al. (Zhang et al., 2019) proposed dividing the weaving segment into N subsegments and transmitting lane-changing advisories to drivers who just reached the subsegment. Their results indicated that the proposed strategy could reduce traffic congestion and improve traffic efficiency. McCoy and Patrick (McCoy and Pesti, 2001) put forward a rule called the dynamic late merge to give the lane-changing position advisory to drivers to reduce accidents and increase the capacity of the weaving segment. Leclercq et al. (Leclercq, Laval and Chiabaut, 2011) proposed an analytical model that extended the Newell-Daganzo model by relating the capacity drop to the merging process, in which two cases were investigated depending on the traffic states on the on-ramp, and the model properties were analyzed and a sensitivity analysis was performed to quantify the relative contribution of each parameter in the capacity drop.

The data analysis-based models give lane-changing advisories to drivers in a weaving segment with a fixed length based on empirical or simulation data analysis. In the models, the starting position of a merge segment is considered the location to set a traffic sign to send a lane-changing advisory. Saad et al. (Saad et al., 2018) developed a log-linear model to explore the relationships between the merging conflict frequency and the length of the weaving segment. They found that a length of 305 m per lane-changing was the optimal length of the weaving segment before an off-ramp. He et al. (He et al., 2020) investigated the relationship between the average travel time and the lane-changing advisory position before an accident site by simulations, which aimed to avoid secondary accidents and reduce traffic congestion when there was a lane-closure problem due to the accident. Yuan et al. (Yuan et al., 2019) analyzed the effect of the length of the weaving segment on driver lane-changing behavior based on experimental data, which revealed that an optimal length of the weaving segment existed. Gong and Du (Gong and Du, 2016) proposed a mathematical model to calculate the optimal location of lane-changing advisory before an off-ramp. In the paper, the delay and fluctuation caused by lane-changing were analyzed from a macro perspective. An optimization model to minimize traffic delay was proposed to search for the optimal location to start a freeway-exiting preparation. However, their study was based on macroscopic analysis and did not consider the characteristics of individual drivers.

2.3. Lane-changing decision before an off-ramp for human drivers

Some studies focused on how human drivers make a lane-changing decision before an off-ramp. Yang and Koutsopoulos (Yang and Koutsopoulos, 1996) presented a microscopic traffic simulator (MITSIM), in which the mandatory lane-changing decision before an off-ramp was investigated, and a fixed distance to the off-ramp was chosen as the freeway-exiting starting point. Zhang et al. (Zhang et al., 2018) investigated the lane-changing decision before an off-ramp by modeling the utility for each alternative lane considering driving route information, traffic environment, and driver characteristics, and the decision of choosing the left lane or right lane was made by evaluating which one had the largest utility. Hao et al. (Hao et al., 2020) studied the relationship between the lane-changing intention of a driver before an off-ramp and the drivers' MLC pressure that was a linear function of the vehicle position, the number of lanes that need to be crossed, and the average arrival rate of vehicles. Vechione et al. (Vechione, Balal and Cheu, 2018) investigated the key factors that had a significant impact on the MLC decision before an off-ramp based on the empirical data analysis.

2.4. Summary

The reviews on the existing studies related to this paper are summarized as follows,

(1) The existing studies on the mandatory lane-changing of AVs made full use of the AV's perception ability and its controllability to propose the mandatory lane-changing model on the microscopic level, aiming to decide whether the target lane is safe for a

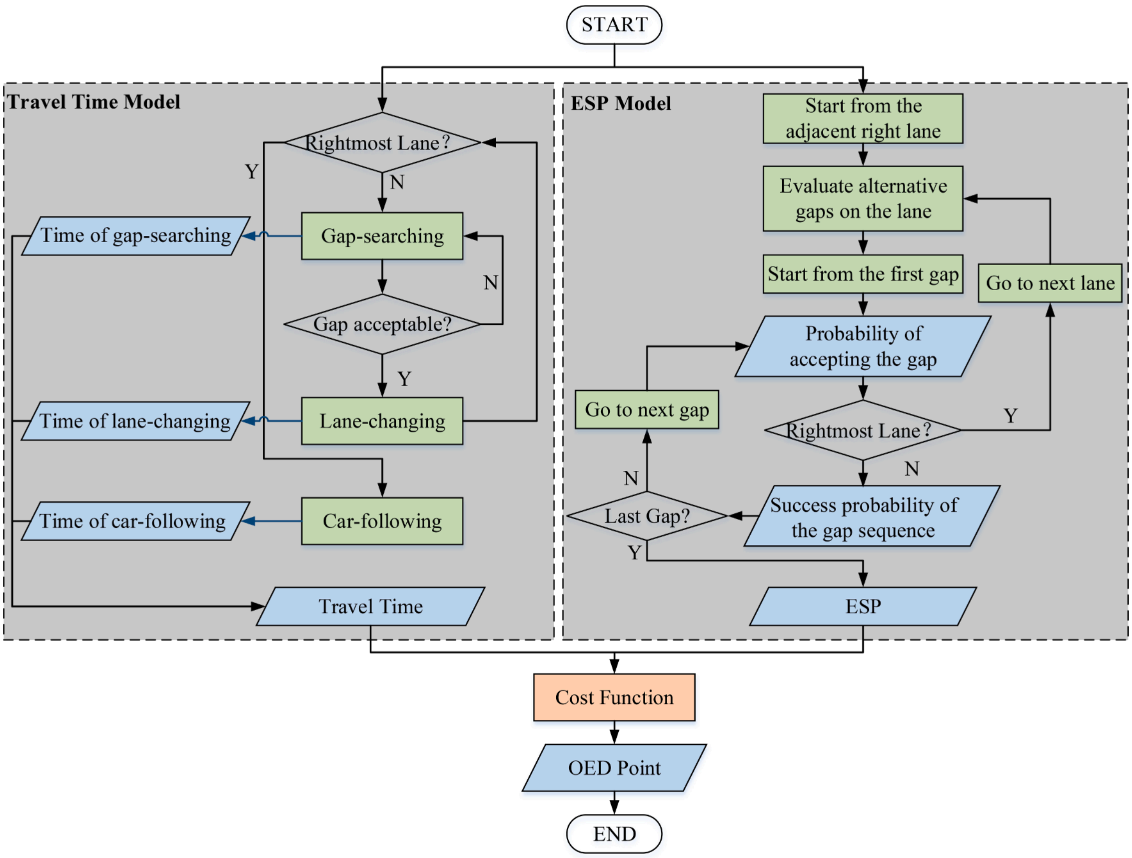

Fig. 2. Framework of the proposed methodology

lane-changing, when/where to execute a lane-changing, and the gap on the target lane can be accepted. However, they did not provide directly mathematical methods and models for the OED problem this paper focused on.

(2) The existing studies on the lane-changing advisory models adopted simple control rules or empirical experience to guide the whole or part of the traffic flow to merge at a fixed point, aiming to reduce traffic delay. These methods are not precise enough to conduct individual vehicle control for AVs.

(3) The existing studies on the lane-changing decision before an off-ramp for human drivers still belonged to the traditional MLC decision of human drivers and tried to help drivers to increase the success possibility in an MLC process. The studies did not try to find an optimal point to start the freeway-exiting process.

Therefore, both the related studies for AVs and human drivers did not provide directly transferrable methods and models for the targeted research problem in this paper, and the novel model should be proposed.

Table 1
Variables and notations

Variables	Descriptions
J	cost function
J_1	driving efficiency
J_2	unsuccess probability of the freeway-exiting
ω	weight value in the cost function
T	travel time of the AV in the freeway-exiting process
$T_{\max}$	maximum value of T
P	ESP of the AV
P_0	minimum value of ESP
N	lane number that the AV is located at first
n	n-th lane on the freeway, and $1 < n \le N$
$\Gamma ss\ n$	time of searching for a safe lane-changing gap on Lane n
$\Gamma se\ n$	time of executing a lane-changing from Lane n to Lane n-1
Γ^{cf}	time of driving on Lane 1
Γ_n	time that the AV can use to find an acceptable lane-changing gap on Lane n
S_n	longitudinal distance that the AV can use to search for an acceptable lane-changing gap on Lane n (n>1)
S_1	longitudinal distance that the AV drives on Lane 1
SA_n	longitudinal distance from the freeway-exiting decision position to LLP on Lane n
SE_n	total longitudinal distance of the lane-changing trajectories from Lane N to Lane n
SS_n	total longitudinal distance of searching for acceptable gaps from Lane N to Lane n
S'_n	relative displacement between the AV on Lane n and the traffic flow on Lane n-1
se_n	longitudinal distance of the lane-changing trajectory from Lane n to Lane n-1
ss_n	longitudinal distance of searching for an acceptable gap on Lane n-1
y	lateral position of the AV during a lane-changing
x	longitudinal position of the AV during a lane-changing
a_i	coefficients of the polynomial function of the lane-changing trajectory
y_{end}	lateral position of the endpoint of the lane-changing trajectory
x_{end}	longitudinal position of the endpoint of the lane-changing trajectory
$x$max end	maximum longitudinal distance of lane-changings in all trajectories
J_{LC}	cost function in a lane-changing trajectory planning process
ξ	weight value in the cost function in a lane-changing trajectory process
as end	side acceleration at the final position of the lane-changing trajectory
as max	maximum safe side acceleration of the lane-changing trajectory
t^{LC}	time used to finish the lane-changing execution
tLC max	maximum lane-changing time
v_{end}	speed of the AV at the final position of the lane-changing trajectory
$K(x)$	curvature function of the lane-changing trajectory concerning for the longitudinal position
$y'(x)$	first derivative of the lane-changing trajectory function
$y''(x)$	second derivative of the lane-changing trajectory function
v_n	speed of the AV on Lane n
v'_n	speed of the AV changing from Lane n to Lane n-1
$\overline{v}_n$	average speed of the vehicles on Lane n
m_n	the m_n-th gap on Lane n
$h_{m_{n-1}}$	the m-th gap on Lane n-1
$E_n(h)$	expectation of the headway values on Lane n
p_n	probability that the gap on Lane n -1 can satisfy the lane-changing safety requirement
$f_n(h)$	time headway distribution on Lane n
$F_n(h)$	cumulative distribution function of the time headway distribution on Lane n
H_{safe}	safe lane-changing time gap
M_n	number of gaps that the AV can meet on Lane n before LLP (latest lane-changing point)
$E_n\ (h)$	expected value of the time headways of the vehicles on Lane n
$p_{m_{n-1}}$	probability that the m-th gap on Lane n-1 is accepted
Γ_n	time that the AV can use to find an acceptable lane-changing gap on Lane n-1

3. Methodology

The methodology is proposed in this section. The framework of the optimal exiting position decision model is proposed first. Following that, the two key variables in the OED model, the travel time and ESP, are modeled respectively. Moreover, the mathematical solution of the proposed model is analyzed, and the two-lane scenario is taken as an example to demonstrate the existence and uniqueness of the solution.

3.1. Optimal exiting decision point model

A further freeway-exiting decision position can increase the success probability and safety but will decrease the driving efficiency of the AV due to its earlier entering into a slower lane. Thus, an optimal freeway-exiting decision position exists for the AV in a freeway-exiting process, which should be able to balance the success probability and driving efficiency. The framework of the proposed methodology to solve the problem of the freeway-exiting decision position is displayed in Fig. 2. In the proposed methodology, an objective function is constructed to comprehensively evaluate the total cost of the AV in a freeway-existing process. By minimizing the cost function, the OED point can be derived. In the cost function, the two key variables, the travel time used to leave the freeway and the exiting success probability (ESP), need to be obtained for a specific exiting decision point. Thus, the two models to calculate the travel time and ESP are proposed respectively. The travel time in a freeway-exiting process consists of the gap-searching time on the current lane, the lane-changing time from the current lane to the target lane, and the car-following time on the outmost lane. ESP can be obtained by evaluating the probability that each gap on the right lane can be accepted and the probabilities of all the feasible lane-changing gap sequences on the right lanes. Variables appeared in the proposed methodology and their descriptions are summarized in Table 1.

Finding the optimal freeway-exiting decision point can be summarized as an optimization problem in which the objective function is the total cost of the AV in the freeway-exiting process, weighting the success probability and efficiency, as follows,

$$\min J = \omega J_1 + (1-\omega) J_2 \tag{1}$$

where J denotes the cost function, J_1 denotes the driving efficiency, J_2 denotes the unsuccess probability of freeway-exiting, and ω denotes the weight value.

In the cost function, the travel time is used to represent efficiency, and ESP is used to represent safety. The two parts of the cost function are calculated as follows,

$$J_1 = T / T_{\max} \tag{2}$$

$$J_2 = 1 - P \tag{3}$$

where T denotes the travel time of the AV in the freeway-exiting process, $T_{\max}$ denotes the maximum value of T, and P denotes the ESP.

The constraints for the optimization problem are as follows,

$$P_0 \le P < 1 \tag{4}$$

$$0 \le \omega \le 1 \tag{5}$$

where P_0 denotes the minimum value of the ESP.

The OED point can be derived by minimizing the cost function with the constraints. In the optimization problem, the efficiency decreases with the increment of the distance to the ramp, but the success probability has the opposite trend, so an optimal solution exit for the problem. The two variables in the objective function, the travel time and success probability, will be modeled and calculated in

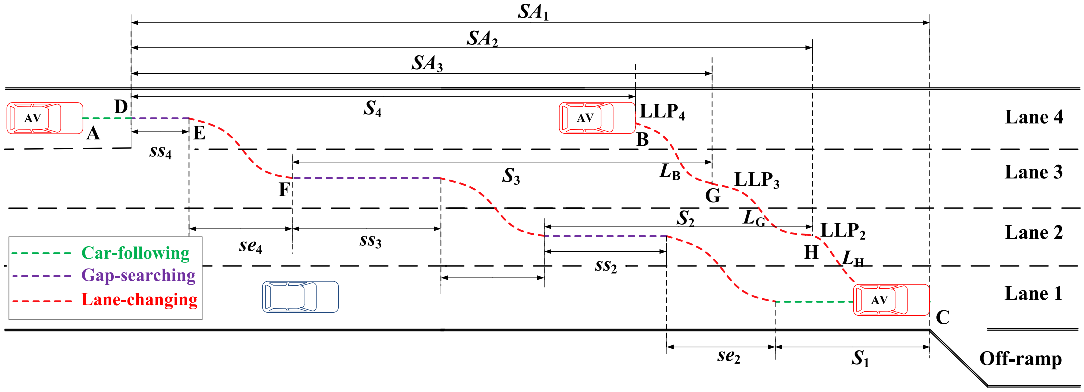

Fig. 3. Detailed freeway-exiting process of an AV

the following subsections.

3.2. Estimation for the travel time in the freeway-exiting process

The relationship between the travel time and the position of the exiting decision point is analyzed and modeled in this subsection Fig. 3. illustrates the detailed freeway-exiting process of an AV, in which the AV is located at position A at first and has to arrive at point C before entering into the off-ramp. Assuming that the AV makes a freeway-exiting decision at point D, SA_1 between points C and D will be the space that can be used to conduct the freeway-leaving process for the AV. The whole freeway-exiting process consists of a series of "gap-searching & lane-changing" processes from Lane N to Lane 2 and a car-following process on Lane 1. If an acceptable gap is found at point E, the AV will change a lane and move to point F. Following that, the AV repeats the "gap-searching & lane-changing" until the AV reaches Lane 1 and then moves to point C to exit the freeway. It should be noted that the gap-searching period (ss_i) can be zero in the process, which means point E can overlap with point D if an acceptable gap is found immediately once the AV generates a freeway-exiting intention.

Since the lane-changing process needs a longitudinal space, there is the latest position on Lane 2 to execute a lane-changing for the AV to make sure it can reach Lane 1 before point C and leave the freeway successfully. point B is defined as the latest lane-changing point (LLP) for the AV on Lane 2. Similarly, on Lane 3 and Lane 4, the LLPs also exit for the AV. In Fig. 3, L_B, L_G, and L_H (the curve from point B to point C) represent three continuous lane-changing trajectories of the AV, which is a connection of the three latest lane-changing trajectories. If the AV starts changing a lane after point B, it will be impossible for the AV to exit the freeway. Thus, point B is the latest position to start the freeway-exiting process in this case, and the longitudinal distance from D to B (S_4 in Fig. 3) is the theoretical space that the AV can use to make a freeway-exiting decision.

According to the above analysis on the freeway-exiting process, the travel time of the AV in the freeway-exiting process can be calculated as follows,

$$T = \sum_{k=2}^{N} \Gamma_k^{ss} + \sum_{k=2}^{N} \Gamma_k^{se} + \Gamma^{cf} \tag{6}$$

where N denotes the lane number that the AV is located at first, which is 4 in Fig. 3, $\Gamma ss\ k$ denotes the time of searching for a safe lane-changing gap on Lane k, $\Gamma se\ k$ denotes the time of executing a lane-changing from Lane k to Lane k-1, and Γ^{cf} denotes the time of driving on Lane 1.

The travel times in the gap-searching, lane-changing, and car-following processes are calculated as follows,

$$\Gamma_k^{ss} = \frac{ss_k}{v_k} \tag{7}$$

$$\Gamma_k^{se} = \frac{se_k}{v'_k} \tag{8}$$

$$\Gamma^{cf} = \frac{S_1}{v_1} \tag{9}$$

where ss_k denotes the longitudinal distance of searching for an acceptable gap on Lane k-1, v_k denotes the speed of the AV on Lane n, se_k denotes the longitudinal distance of the lane-changing trajectory from Lane k to Lane k-1, v'_k denotes the speed of the AV when changing from Lane k to Lane k-1, and S_1 denotes the longitudinal distance that the AV drives on Lane 1.

According to Fig. 3, the longitudinal distance S_n that the AV can use to search for an acceptable time gap on Lane n (n>1) can be calculated as follows,

$$S_n = SA_n - SE_n - SS_n \tag{10}$$

where SA_n denotes the longitudinal distance from the freeway-exiting decision position to LLP on Lane n, SE_n denotes the total longitudinal distance of the lane-changing trajectories from Lane N to Lane n, and SS_n denotes the total longitudinal distance of searching for an acceptable gap from Lane N to Lane n.

In Eq. (10), SE_n and SS_n can be calculated as follows,

$$SE_n = \sum_{k=n+1}^{N} se_k \tag{11}$$

$$SS_n = \sum_{k=n+1}^{N} ss_k \tag{12}$$

The relative displacement S_n' between the AV on Lane n and traffic flow on Lane n-1 in time $\Gamma ss\ n$ can be derived as follows,

$$S'_n = |\overline{v}_{n-1} - v_n| \cdot \Gamma_n^{ss} = |\overline{v}_{n-1} - v_n| \cdot \frac{ss_n}{v_n} \tag{13}$$

where $\overline{v}_n$ denotes the average speed of the vehicles on Lane n.

When the AV travels on Lane n, assuming the $m_{n\text{-}1}$-th gap on Lane n-1 is accepted by the AV, $S_n{}'$ can be calculated as follows,

$$S_n^{'} = m_{n-1} \cdot [(h_1 + h_2 + h_3 + \cdots h_{m_{n-1}}) / m_{n-1}] \cdot \overline{v}_{n-1} = (m_{n-1} - 1) \cdot E_{n-1}(h) \cdot \overline{v}_{n-1} \tag{14}$$

where $h_{m_{n-1}}$ denotes the m-th gap on Lang n-1, $E_{n\text{-}1}(h)$ denotes the expectation of headway values on Lane n-1, and $\overline{v}_{n-1}$ denotes the average speed of the vehicles on Lane n-1.

Thus, ss_n can be calculated as follows,

$$ss_n = \frac{S^{'}{}_n \cdot \overline{v}_n}{|\overline{v}_n - \overline{v}_{n-1}|} = \frac{(m_{n-1} - 1) \cdot E_{n-1}(h) \cdot \overline{v}_{n-1} \cdot \overline{v}_n}{|\overline{v}_n - \overline{v}_{n-1}|} \tag{15}$$

The lane-changing trajectory has been well studied by the existing studies, so the trajectory of lane-changing can be obtained by the method presented in the paper (Yang et al., 2018). The following polynomial function is used to represent the lane-changing trajectory curve,

$$y(x) = a_0 + a_1 x + a_2 x^2 + a_3 x^3 \tag{16}$$

where a_0, a_1, a_2, and a_3 respectively denote the coefficients of the polynomial function, x denotes the longitudinal position of the AV during a lane-changing, and y denotes the lateral position of the AV during a lane-changing.

Taking L_B as an example, the lane-changing trajectory starts from B and ends at G. The course angle of the AV at B is zero, and it will change with the movement of the AV from B to G and go back to zero at G. Assuming that the coordinate is (0, 0) at the starting point B and is (x_{end}, y_{end}) at the endpoint G, there is,

$$y^{'}(0) = 0 \tag{17}$$

$$y^{'}(x_{\text{end}}) = 0 \tag{18}$$

where $y'(x)$ denotes the first derivative of the lane-changing trajectory function.

Replacing $y(x)$ in Eqs. (17) and (18) with Eq. (16), and solving the functions produce,

$$a_1 = 0 \tag{19}$$

$$a_0 = 0 \tag{20}$$

$$a_2 = \frac{3y_{\text{end}}}{x_{\text{end}}^2} \tag{21}$$

$$a_3 = \frac{-2y_{\text{end}}}{x_{\text{end}}^3} \tag{22}$$

Replacing the parameters a_0, a_1, a_2 and a_3 in Eq. (16) with Eqs. (19)-(22) produces,

$$y(x) = \frac{3y_{\text{end}}}{x_{\text{end}}^2} x^2 - \frac{2y_{\text{end}}}{x_{\text{end}}^3} x^3 \tag{23}$$

Eq. (23) is the lane-changing trajectory for the AV in a freeway-exiting process. If a consecutive lane-changing crossing multiple lanes happens, it can be decomposed into several lane-changing trajectories of Eq. (23). Moreover, in Eq. (23), y_{end} equals the width of the lane, and it is a constant, so the trajectory is uniquely determined by the longitudinal ending position x_{end}. Two factors, efficiency and comfort, should be taken into account simultaneously to find an optimal trajectory. Efficiency and comfort are two mutually contradictory factors, so the optimal lane-changing trajectory should balance them. A cost function is adopted to describe how comfort and efficiency impact the optimal lane-changing trajectory of automated vehicles. The equation of the cost function is as follows,

$$J_{\text{LC}} = \xi \left(a_{\text{end}}^s / a_{\max}^s \right)^2 + (1 - \xi) t^{\text{LC}} / t_{\max}^{\text{LC}} \tag{24}$$

where J_{LC} denotes the cost function in a lane-changing trajectory process, *as* end denotes the side acceleration at the final position of the lane-changing trajectory, *as* max denotes the maximum safe side acceleration of the lane-changing trajectory, t^{LC} denotes the time used to finish the lane-changing execution, *t*LC max denotes the maximum lane-changing time, and ξ is a weight value in the cost function in a lane-changing trajectory process.

In Eq. (24), the side acceleration at the final position *as* end obtains the maximum side acceleration for a given lane-changing trajectory curve, so it can represent the lane-changing comfort for passengers. The time used in a lane-changing process can reflect the lane-changing efficiency. The greater t^{LC} indicates the lower efficiency.

The side acceleration at the final position *as* end can be calculated by the following equation,

$$a_{\text{end}}^s = v_{\text{end}}^2 K(x_{\text{end}}) \tag{25}$$

where v_{end} denotes the velocity of the AV at the final position of the lane-changing trajectory, and $K(x)$ denotes the curvature function of the lane-changing trajectory concerning the longitudinal position, which can be calculated by the following equation,

$$K(x) = \left| y''(x) \Big/ \left(1 + (y'(x))^2\right)^{\frac{3}{2}} \right| \tag{26}$$

where $y''(x)$ denotes the second derivative of the lane-changing trajectory function.

Replacing $y'(x)$ and $y''(x)$ in Eq. (26),

$$K(x) = \left| \left(\frac{6y_{\text{end}}}{x_{\text{end}}^2} - \frac{12y_{\text{end}}}{x_{\text{end}}^3} x \right) \Big/ \left(1 + \left(\frac{6y_{\text{end}}}{x_{\text{end}}^2} x - \frac{6y_{\text{end}}}{x_{\text{end}}^3} x^2 \right)^2 \right)^{\frac{3}{2}} \right| \tag{27}$$

With the change of x, the curvature of trajectory first decreases to zero and then increases to the maximum value at the end of the lane-changing. The maximum curvature locates at the ending point of the lane-changing trajectory, so Eq. (25) has the following form,

$$a_{\text{end}}^s = v_{\text{end}}^2 \left| \frac{6y_{\text{end}}}{x_{\text{end}}^2} \right| \tag{28}$$

Therefore, the final expression of the cost function J_{LC} of the lane-changing is as follows,

$$J_{\text{LC}} = \xi \left(v_{\text{end}}^2 \left| \frac{6y_{\text{end}}}{x_{\text{end}}^2} \right| \Big/ a_{\max}^s \right)^2 + (1-\xi) \frac{t^{\text{LC}}}{t_{\max}^{\text{LC}}} = \xi \left(v_{\text{end}}^2 \left| \frac{6y_{\text{end}}}{x_{\text{end}}^2} \right| \Big/ a_{\max}^s \right)^2 + (1-\xi) \frac{x_{\text{end}}}{x_{\text{end}}^{\max}} \tag{29}$$

where $x$max end denotes the maximum longitudinal distance of lane-changings in all trajectories.

In Eq. (29), the cost function J_{LC} is a function concerning for x_{end}, and the x_{end} producing the minimum J is the longitudinal position of the optimal trajectory x. By solving Eq. (29), the trajectory L_{LC} can be obtained, and thus se_2 can be obtained as well.

Thus, replacing SE_n and SS_n in Eq. (10) with Eqs. (11), (12), and (15), we can obtain S_n, based on which the longitudinal distance in the car-following process can be derived as follows,

$$S_n = SA_n - \sum_{k=n+1}^{N} se_k - \sum_{k=n+1}^{N} \frac{(m_{k-1} - 1) \cdot E_{k-1}(h) \cdot \bar{v}_{k-1} \cdot \bar{v}_k}{|\bar{v}_k - \bar{v}_{k-1}|} \tag{30}$$

3.3. *Exiting success probability model*

3.3.1. *Two-lane scenario*

This subsection aims to establish a relationship between ESP and the distance of the decision point to the off-ramp Fig. 4. displays a freeway-exiting process of an AV on a two-lane freeway. In the figure, an AV is currently located at point A on the left lane and will exit the freeway from the off-ramp. Assuming the AV makes a freeway-exiting decision at point D. According to Subsection 3.2, S_2 (the longitudinal distance between points D and B) is the space the AV can use to search for an acceptable time gap to conduct a safe lane-changing from Lane 2 to Lane 1. If an acceptable gap is found at point E, the AV will move to point F following the curve L_{E} and then drives to point C to exit the freeway.

S_2 has a significant impact on the number of safe lane-changing gaps the AV can meet and further influences the value of ESP. The closer the freeway-exiting decision position to the off-ramp is, the smaller the value of ESP is. In addition to the position of the exiting decision point, the LLP point and the gap distribution of the traffic flow are also critical variables to determine the value of ESP, so they are also should be considered in the proposed model.

After the AV on Lane 2 generates a freeway-exiting intention, it begins to search for a safe gap to conduct a lane-changing to Lane 1. In the searching process, the AV judges whether the next gap satisfies the safety requirements for a lane-changing until it meets a qualified gap. As shown in Fig. 5, the AV can meet 6 gaps, and 3 of them satisfy the safe lane-changing condition. The probability of successfully changing a lane (that is ESP for the two-lane case) can be calculated as follows,

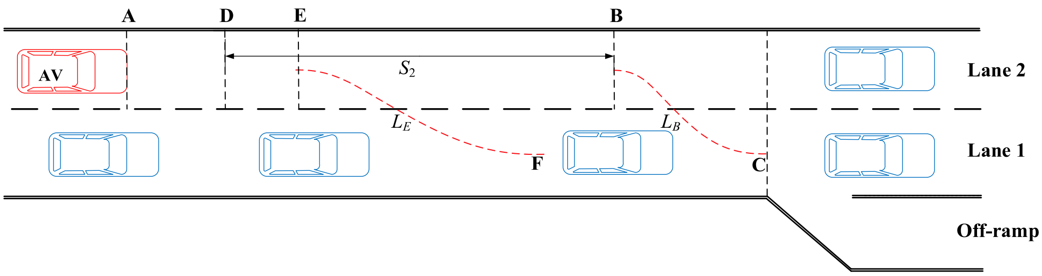

Fig. 4. Freeway-exiting process for an AV on a two-lane freeway

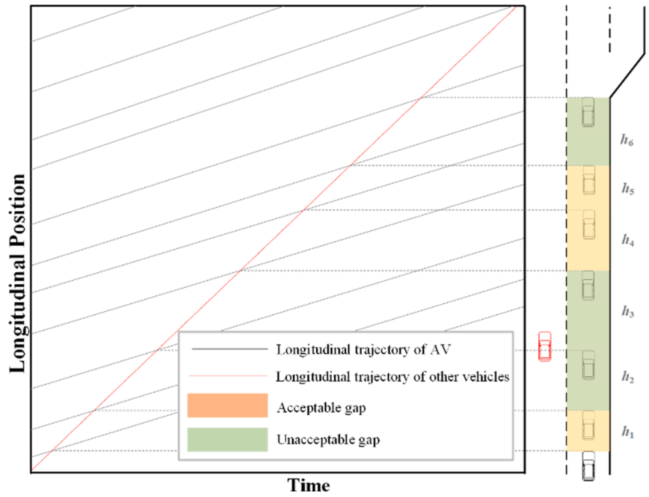

Fig. 5. Schematic of the gap that the AV may meet when leaving a two-lane freeway

$$P = 1 - (1 - p_2)^{M_1} \tag{31}$$

where P denotes ESP of the AV, p_2 denotes the probability that the gap on Lane 1 can satisfy the lane-changing safety requirement, and M_1 denotes the number of the gaps that the AV can meet on Lane 1 before the LLP.

Therefore, to obtain P, it needs to calculate the probability p_2 and the number of gaps M_1 that the AV can meet in the remaining distance to LLP. The following equation can derive the probability of accepting a gap p_2 as follows,

$$p_2 = 1 - F_1(H_{\text{safe}}) = 1 - \int_0^{H_{\text{safe}}} f_1(h)dh \tag{32}$$

where $f_1(h)$ denotes the time headway distribution on Lane 1, which can be chosen according to the traffic state, F_1 denotes the cumulative distribution function of the time headway distribution on Lane 1, and H_{safe} denotes the safe lane-changing time gap, whose value in calculation can refers to the study of Yang et al. (Yang, Wang and Quddus, 2019).

Replacing p_2 in Eq. (31) with Eq. (32) produces,

$$P = 1 - \left(\int_0^{H_{\text{safe}}} f_1(h)dh \right)^{M_1} \tag{33}$$

From Eq. (14) and Eq. (13), we can use the expected value of headways and the average speed to estimate the number of gaps M_1 that the AV can meet on Lane 1 in the remaining distance, that is,

$$M_1 = \frac{|\bar{v}_1 - v_2| \cdot S_2}{E_1(h) \cdot \bar{v}_1 \cdot v_2} \tag{34}$$

Replacing M_1 in Eq. (33) with Eq. (34), the ESP for the two-lane freeway can be derived as follows,

$$P = 1 - \left(\int_0^{H_{\text{safe}}} f_1(h)dh \right)^{\frac{|\bar{v}_1 - v_2| \cdot S_2}{E_1(h) \cdot \bar{v}_1 \cdot v_2}} \tag{35}$$

Once a freeway-exiting decision point is generated, S_2 and v_2 can be determined, and $f_1(h)$, $E_1(h)$, and $\bar{v}_1$ can be easily determined by the distribution of the headways on Lane 1. Therefore, the proposed model can obtain the value of ESP at a given position. It can be seen that the ESP depends on the headway distribution $f_1(h)$, the average speed of vehicles on Lane 1, and the distance to the LLP (or the distance to the off-ramp).

3.3.2. Multi-lane scenario

This subsection focuses on the general freeway-exiting position decision model of AVs for the multi-lane scenario. In the multi-lane scenario, the AV needs multiple lane-changing movements to reach the outmost lane. The multilane scenario is much more complex than the two-lane scenario in calculating ESP. The freeway-exiting process in the two-lane scenario can be simply regarded as a problem of calculating the successful lane-changing probability from Lane 2 to Lane 1 before the AV reaches the latest lane-changing point. However, for the multi-lane scenario, the freeway-exiting process consists of multiple times of lane-changings, and a different early chosen lane-changing gap will result in different alternative gaps on the remaining lanes. Thus, in the multi-lane scenario, it more cares about a "gap sequence" for the lane-changing. The success probability of each "gap sequence" needs to be calculated, and the total ESP is the sum of the success probabilities of a series of "gap sequences".

Taking the case of four lanes in Fig. 3 as an example, the AV locates at point A on Lane 4 at first, and to reach the off-ramp, the AV needs to change to Lane 3, Lane 2, and Lane 1 gradually. Point B is the LLP on Lane 4, from which the AV changes to Lane 3 following the lane-changing trajectory curve L_B first, subsequently changes to Lane 2 following L_G, and finally changes to Lane 1 following L_H. If the AV generates a freeway-exiting decision at point D and finds an acceptable gap at point E, the AV will be able to change to Lane 3. After the AV arrives at point F on Lane 3, it will repeat the process of searching for an acceptable gap and try to change to Lane 2 and Lane 1. If the AV can successfully change to Lane 1 before point C, it can leave the freeway by the off-ramp successfully; otherwise, it fails to leave the freeway.

In the four-lane scenario, the LLP (B) on Lane 4, the LLP (G) on Lane 3, and the LLP (H) on Lane 2 can be also determined by applying the lane-changing trajectory planning method (Yang et al., 2018). Assuming the total number of lanes is N, to calculate the position of point B, the lane-changing trajectory planning method needs to be applied for N-1 times. The different lanes on a freeway have different average speeds, and the average speed gradually increases as moving outside and is the lowest on the outmost lane, because the outer lanes are closer to the off-ramp and have more frequent lane-changings.

Assume the AV is located on Lane n ($1 < n \leq N$) and decides to exit the freeway by the closest off-ramp, and S_n is the distance between the decision position to the LLP on Lane n, so the probability that the m_{n-1}-th gap on Lane n-1 is accepted can be calculated by the following equation,

$$p_{m_{n-1}} = (1 - p_n)^{m_{n-1}-1} \cdot p_n, m_{n-1} = 1, 2\cdots, M_{n-1} \tag{36}$$

where $p_{m_{n-1}}$ denotes the probability that the m-th gap on Lane n-1 is accepted, M_{n-1} denotes the number of gaps that the AV can meet on Lane n-1, and p_n denotes the probability that the gap Lane n-1 is acceptable.

In Eq. (36), the number of gaps that the AV can meet on Lane n-1 can be determined by the position of the freeway-exiting decision position on Lane n, which means M_{n-1} is a function of S_n, as follows,

$$M_{n-1} = g(S_n) \tag{37}$$

With a given distribution of the headway on Lane n-1, p_n can be easily derived as follows,

$$p_n = 1 - F_{n-1}\left(H_{\text{safe}}\right) = 1 - \int_0^{H_{\text{safe}}} f_{n-1}(h)dh \tag{38}$$

where $f_{n-1}(h)$ denotes the time headway distribution on Lane n-1, and F_{n-1} denotes the cumulative distribution function of the time headway distribution.

Once the AV has changed to Lane n-1, it will begin to search for a new acceptable lane-changing gap on Lane n-2 immediately, so the lane-changing finishing point on Lane n-1 is the freeway-exiting decision position for Lane n-2. The process is repeated until the AV reaches Lane 1.

Adopting the same method of the two-lane scenario, the number M_{n-1} of the gaps that the AV can meet on Lane n-1 in the multi-lane scenario is derived as follows,

$$M_{n-1} = \frac{|\overline{v}_n - \overline{v}_{n-1}| \cdot \Gamma_n}{E_{n-1} \cdot \overline{v}_{n-1}} \tag{39}$$

where Γ_n denotes the time that the AV can use to find the acceptable gap for lane-changing and can be obtained by the following equation,

$$\Gamma_n = \frac{S_n}{v_n} \tag{40}$$

The number of gaps on Lane n-1 that the AV can meet on Lane n-1 is as follows,

$$M_{n-1} = \frac{|\overline{v}_n - \overline{v}_{n-1}| \cdot \left(SA_n - \sum_{k=n+1}^{N} SE_k - \sum_{k=n+1}^{N} \frac{(m_{k-1}-1)\cdot E_{k-1}(h)\cdot \overline{v}_{k-1}\cdot \overline{v}_k}{|\overline{v}_k - \overline{v}_{k-1}|} \right)}{E_{n-1}(h) \cdot v_n \cdot \overline{v}_{n-1}} \tag{41}$$

Furthermore, if the AV arrives at Lane n-1 and intends to change to Lane n-2, S_{n-1} is determined by both S_n and the chosen gap j_{n-1} on Lane n-1. Therefore, in the entire process from generating a decision to leaving the freeway, the following recurrence relationship is met,

$$\begin{cases} S_{n-1} = f(S_n, m_{n-1}) \\ M_{n-1} = g(S_n) \end{cases}, n = N, N-1, \cdots, 2 \tag{42}$$

Thus, for a given freeway-exiting path following the feasible gap sequence $m_1, \ldots m_{N-1}$, the ESP function for the multi-lane freeway can be derived as follows,

$$P = \sum_{m_1 \in \{1,2,\ldots,M_1\},\cdots,m_{N-1} \in \{1,2,\ldots,M_{N-1}\}} \Pr(m_1, \cdots, m_{N-1}) = \sum_{m_1 \in \{1,2,\ldots,M_1\},\cdots,m_{N-1} \in \{1,2,\ldots,M_{N-1}\}} \prod_{n=2}^{N} p_{m_{n-1}} \tag{43}$$

An example of calculating ESP for the multi-lane scenario is illustrated in Fig. 6, in which it is assumed that the AV driving on Lane 5 produces a freeway-exiting intention and will meet 4 alternative gaps on the right lane (Lane 4) during the remaining travel time Γ_5 ($M_4 = 4$). The numbers in circles represent the gap orders that the AV can meet on each lane. The tree structure in Fig. 7 represents all the possible situations in the freeway-exiting process. The green solid lines represent the feasible gap sequences by which the AV can leave the freeway successfully. The red dotted lines represent the sequences that cannot lead the AV to exit the freeway, whose ESPs are 0. The ESP in this example is the sum of the success probabilities of the five successful sequences, and Eq. (43) can be written as follows,

$$p = p_{m_4=1}p_{m_3=1}p_{m_2=1}p_{m_1} + p_{m_4=1}p_{m_3=1}p_{m_2=2}p_{m_1} + p_{m_4=1}p_{m_3=2}p_{m_2=1}p_{m_1} + p_{m_4=2}p_{m_3=1}p_{m_2=1}p_{m_1} \tag{44}$$

3.4. Mathematical analysis on the optimal exiting decision point

In Eq. (1), with the increment of the distance from the freeway-exiting decision position to the off-ramp, the travel time T increases, and the efficiency decreases, which makes the value of cost function J greater. On the other hand, the increment of the distance from the freeway-exiting decision position to the off-ramp raises the value of ESP and reduces the value of 1-P, which makes the cost function J smaller.

The minimum value of the cost function J can be obtained by taking the derivative of J to be zero, and it corresponds to the intersection point of the derivative curves of ωJ_1 and (ω-1)J_2. The Scipy.Optimize of Python is used to get the numerical solutions. The schematic solving process of the OED point for the two-lane case is discussed.

In Eq. (1), the time T for the AV to travel from the freeway-exiting decision position on Lane 2 to the ramp consists of the three parts, the time of searching for an acceptable gap on Lane 1, the time of changing from Lane 2 to Lane 1, and the travel time on Lane 1, that is,

$$T = \Gamma_2^{ss} + \Gamma_2^{se} + \Gamma^{cf} = \frac{ss_2}{v_2} + \frac{se_2}{v'_2} + \frac{S_1}{v_1} \tag{45}$$

where S_1 denotes the longitudinal length from the decision position to the off-ramp, se_2 denotes the longitudinal distance of the lane-changing trajectories in the process of changing from Lane 2 to Lane 1, v'_2 denotes the speed of the AV when changes to Lane 1, ss_2 denotes the total longitudinal length used when the AV is searching for a gap to change from Lane 2 to Lane 1, and v_2 denotes the speed of AV when it is on Lane 2.

In Eq. (45), the relationship between SA_1, S_1, SE_1, and SS_1 is S_1+SE_1+SS_1= SA_1 according to Eq. (10). SE_1 and SS_1 can be easily obtained by the traffic condition and headway distribution on Lane 1, and SA_1 can be determined once the freeway-exiting decision position is generated, so the value of S_1 can be obtained. Thus, the derivative of J_1 is as follows,

$$J_1'(SA_1) = 1 / (T_{\max} \cdot v_1) \tag{46}$$

Moreover, in the two-lane case, the function of P is Eq. (35), and the derivative of J_2 is as follows,

$$J_2'(SA_1) = -\frac{|\overline{v}_1 - v_2|}{E_1(t) \cdot \overline{v}_1 \cdot v_2} \cdot \ln\left(F_1\left(H_{\mathrm{safe}}\right)\right) F_1\left(H_{\mathrm{safe}}\right)^{\frac{|\overline{v}_1 - v_2| SA_1}{E_1(t) \cdot \overline{v}_1 \cdot v_2}} \tag{47}$$

By analyzing Eqs. (46) and (47), the solution of the proposed OED model for the two-lane scenario is analyzed in Fig. 7 Fig. 7. (a) displays the changes of J_1, J_2, and J with the distance to the off-ramp, and Fig. 7 (b) displays the changes of J'_1, J'_2, and J with the distance to the off-ramp. In Fig. 7 (a), J_1 increases and J_2 decreases with the increment of the position, so they are two competing functions, which reveals that the optimal solutions exit for J. The variation law of the cost function J can be obtained from Fig. 7 (b). Since there are two intersections for the two curves of J'_1 and J'_2, the cost function J will raise before the first intersection, decrease between the two intersections, and increase again after the second intersection, with the increment of position. In addition, the value of

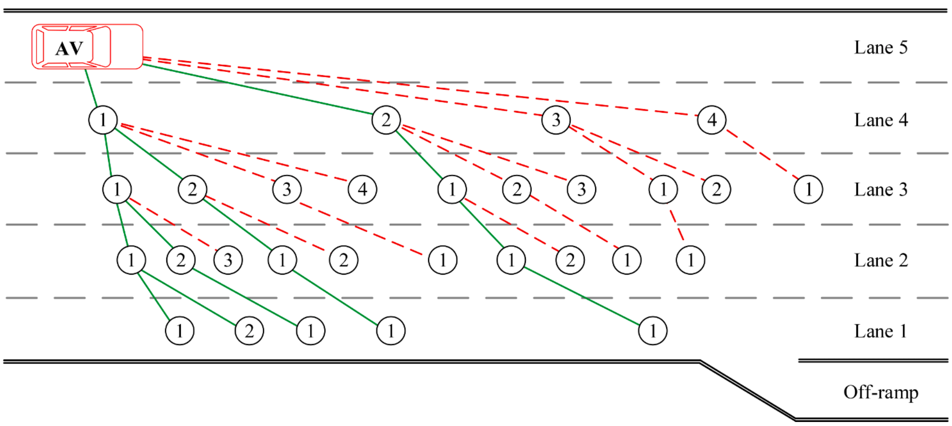

Fig. 6. Example of calculating the ESP for the five-lane scenario

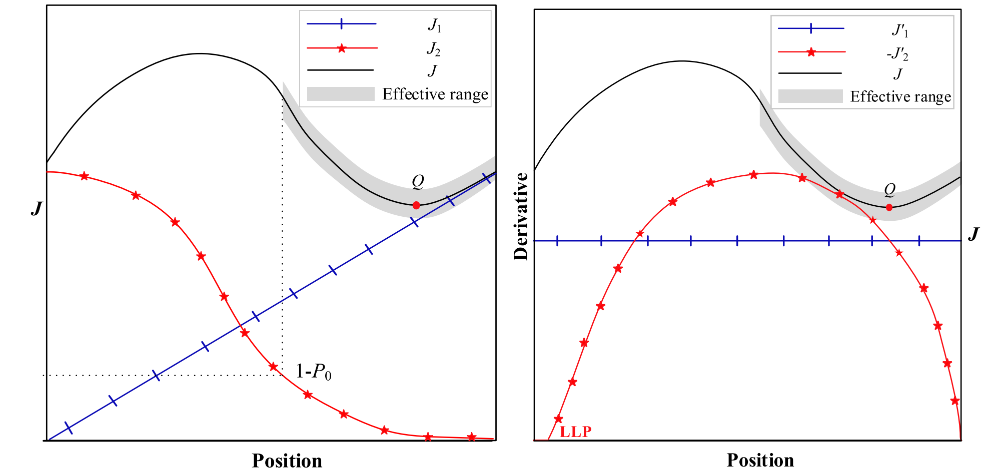

(a) Variations of J_1, J_2, and J with the position **(b) Variations of J'_1, J'_2, and J with position**

Fig. 7. Solution analysis of the proposed OED model for the two-lane scenario

ESP is in the range of [P_0, 1], so there is an effective range for the cost function J (the grey area in the figure). Therefore, the minimum value of the cost function J corresponds to the second intersection point (Point Q in the figure) of the curves of J'_1 and J'_2.

4. Model calibration and validation

In this section, we performed experiments and collected field data on a freeway in Chengdu, China to validate the proposed ESP model. The data collection method is introduced in detail, and the validation results based on the collected data are presented. Moreover, the car-following model is calibrated, and the lane-changing trajectory planning model is evaluated.

4.1. Freeway-exiting position decision model calibration and validation

4.1.1. Data collection

To validate the proposed model, the field experiments were conducted on freeway G401 in Chengdu, China. The selected freeway segment is shown in Fig. 8. In the figure, A_1 and B_1 are the two eastbound on-ramps, B_2, C_1, and C_2 are the three eastbound off-ramps, C_3 and B_4 are the two westbound on-ramps, and B_3, A_2, and A_3 are the three westbound off-ramps.

Since automated vehicles are not allowed to drive on freeways according to the law of China, the testing vehicles used in the experiments were still driven by human drivers. To make that the results of the experiments can simulate the AV as much as possible, it is necessary to ensure that the two testing vehicles can precisely judge their distances to the surrounding vehicles, and the drivers obey the strict safety criteria like AVs in the car-following and lane-changing maneuvers. To realize that, we did the following two jobs. First, a suggestion system based on safe driving models was installed on the vehicles to give driving suggestions to the drivers, in which the sensors including radars and GPS were equipped on the vehicles to accurately estimate the positions and speeds of the testing and surrounding vehicles. In this way, safe driving criteria are guaranteed for the testing vehicles. Second, the volunteer drivers had been trained to obey the suggestions from the driving suggestion system and follow the driving directions to finish the data collection job. It should be noted that although the above jobs make the drivers on the testing vehicles act like AVs as far as possible, the reaction times between the human drivers and real AVs are still different. However, the problem this paper focused on is a decision-making problem whose key influencing factors are the macroscopic characteristics of the traffic flow, such as headway distribution and average traffic speed, so the small difference of reaction times between the human drivers and AVs in experiments will have a negligible effect on the validation results. For the same reason, the difference between the two different testing vehicles will also have not a significant impact on the effectiveness of the validation.

The experiments were performed in two time periods: 8:00 am to 12:00 am and 2:00 pm to 6:00 pm, and the two testing vehicles

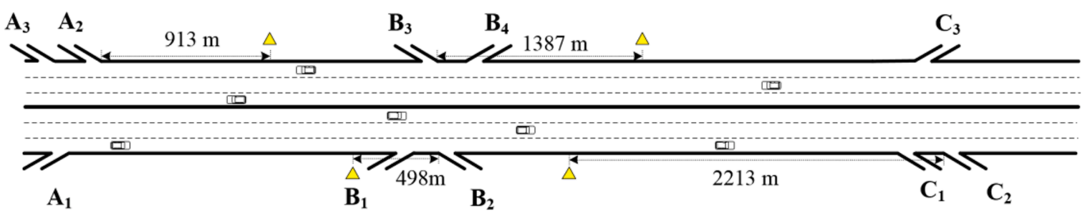

Fig. 8. Selected testing routes on freeway G401

entered into the freeway from the on-ramp C_3 and drove on the testing segments round and round. In addition to the driver, there were two other volunteers in a testing vehicle, including a data logger and a maneuverer to avoid unexpected situations. Some billboards and traffic signs on the freeway were chosen as the freeway-exiting decision points, as the yellow markers shown in Fig. 8. To make full use of the lanes of the freeway, all the testing vehicles drove on the leftmost lane (Lane 3) first and then made freeway-exiting decisions. Once a freeway-exiting intention was generated, the testing vehicle started to search for a safe lane-changing gap and tried to leave the freeway by the closest off-ramp. If the testing vehicle can leave the freeway successfully, we mark the event as a successful freeway-exiting; if a safe lane-changing gap sequence cannot be found until the testing vehicle reached the LLP, the testing vehicle will not be able to leave the freeway successfully, marking the event as a failed freeway-exiting. After multiple tests were conducted, the value of ESP can be obtained for each freeway-exiting decision position. In the end, 103 times of tests were conducted in total. By calculating the numbers of the failed freeway-exiting and successful freeway-exiting, the value of ESP for each yellow marker in Fig. 8 can be obtained, as shown inTable 2.

In addition, cameras were also installed on the roadside to capture the traffic flow data. Five videos were captured in the experiments, and the duration of each video lasted about half an hour.

The headway distributions are extracted from the captured videos, as shown in Table 3. In the table, "Shooting Time" indicates the time that the camera recorded the traffic videos, the time interval for the headway statistics adopts 2 seconds, and the number of vehicles and its corresponding frequency is calculated for each interval. The data in Table 3 will be used to fit several distribution functions to find the best headway distribution function.

4.1.2. Model calibration and validation

Based on the collected data, the proposed models can be validated by comparing the field data with the ESP values calculated by the proposed models. The headway distribution on the target lane is a critical factor to successful freeway-exiting. According to the existing studies (Wu, Hu and Sun, 2010, Singh et al., 2020, Maurya et al., 2016), the headway at different traffic conditions (Peak hour and Non-Peak hour) follows different distributions. The collected headway data is divided into the sub-data for Peak hour and the sub-data for Non-Peak hour to find the best distribution that is the lognormal distribution (Greenberg, 1966), log-logistic distribution (Wu, Hu and Sun, 2010), inverse Gauss distribution (Sun and Benekohal, 2005), and Pearson 3 distribution (Maurya et al., 2016) Fig. 9. exhibits the fitting results, in which the gray histogram is the collected headway data, the colored line respectively represents the fitting results of the distribution functions, and the red line with marker is the best-fitted function.

Table 4 exhibits the fitting errors and the parameters of the five distribution functions, in which μ denotes the means of the distribution functions, and σ denotes the variance of the distribution function. From the fitting results, it can be concluded that the lognormal distribution has the best fitting result in Non-Peak hour, and inverse Gauss distribution performs best in Peak hour, so in the following ESP calculation, the lognormal distribution and inverse Gauss distribution are adopted to simulate the headways in the proposed freeway-exiting position decision model.

With a given distribution function of headway, ESP for a specific position can be calculated using the proposed freeway-exiting position decision model, and the corresponding MAPE (Mean Absolute Percentage Error) can be obtained as well, see Table 5. It can be observed that the MAPE value of the model is less than 13%, which indicates that the proposed model can predict ESP with high accuracy.

4.2. Car-following and lane-changing models calibration and evaluation

In the paper, the Gipps' car-following model (Gipps, 1986) is used to control the longitudinal movement of the AV, and the OpenACC dataset (Makridis et al., 2021) is used to calibrate this model. OpenACC is an Open Database of car-following experiments involving vehicles with Adaptive Cruise Control systems (ACC), whose objective is to provide data about ACC behavior to help the whole scientific community better understand the properties of ACC vehicles. The variables provided by OpenACC are displayed in Table 6. The "Casale dataset" in OpenACC is used to calibrate and validate the Gipps' car-following model, which involves two vehicles and the following vehicle was driving all times with ACC on. The calibration method adopts the one in the reference (Punzo and Simonelli, 2005, Brockfeld, Kühne and Wagner, 2005), and the GA toolbox in MATLAB is applied to find the optimal model parameters. The calibration and validation results are shown in Table 7.

Moreover, the lane-changing trajectory model presented in Subsection 3.2 is evaluated by CarSim, which can analyze vehicle dynamics, develop active controllers, calculate a car's performance characteristics, and engineer active safety systems. CarSim can deliver accurate and detailed methods for simulating the performance of vehicles (Yang et al., 2020). In the simulations, the lane-changing trajectory is generated by the third-order polynomial of Eq. (23), and CarSim is used to evaluate whether the planned

Table 2
Statistical results of ESP in the experiments

Experiments	Number of successful freeway-exiting	Number of failed freeway-exiting	Total number	Success probability	Position of the freeway-exiting decision position (m)
A_1B_2	6	20	26	23.08%	498
B_1C_1	19	6	25	76.00%	2213
C_3B_3	14	10	24	58.33%	1387
B_4A_2	12	16	28	42.85%	913

Table 3
Headway distribution data

	Shooting time 8:00 AM		9:55 AM		10:32 AM		2:00 PM		3:00 PM	
	Duration 28 min		28 min		28 min		24 min		24 min	
Interval (s)	No. (veh)	FREQ (%)	No. (veh)	FREQ (%)	No. (veh)	FREQ (%)	No. (veh)	FREQ (%)	No. (veh)	FREQ (%)
0.5-2.5	90	29.32	89	28.43	93	30.59	52	21.67	38	16.67
2.5-4.5	80	26.06	79	25.24	75	24.67	64	26.67	64	28.07
4.5-6.5	44	14.33	56	17.89	42	13.82	44	18.33	31	13.60
6.5-8.5	29	9.45	31	9.90	35	11.51	32	13.33	35	15.35
8.5-10.5	27	8.79	25	7.99	24	7.89	19	7.92	17	7.46
10.5-12.5	15	4.89	11	3.51	12	3.95	11	4.58	18	7.89
12.5-14.5	10	3.26	5	1.60	6	1.97	6	2.50	7	3.07
14.5-16.5	4	1.30	6	1.92	5	1.64	5	2.08	9	3.95
16.5-18.5	1	0.33	2	0.64	5	1.64	4	1.67	4	1.75
18.5-20.5	1	0.33	2	0.64	2	0.66	0	0.00	4	1.75
20.5-22.5	2	0.65	3	0.96	2	0.66	1	0.42	0	0.00
22.5-24.5	2	0.65	2	0.64	0	0.00	0	0.00	1	0.44
24.5-26.5	1	0.33	1	0.32	0	0.00	1	0.42	0	0.00
26.5-28.5	1	0.33	1	0.32	2	0.66	0	0.00	0	0.00
28.5-30.5	0	0.00	0	0.00	1	0.33	1	0.42	0	0.00

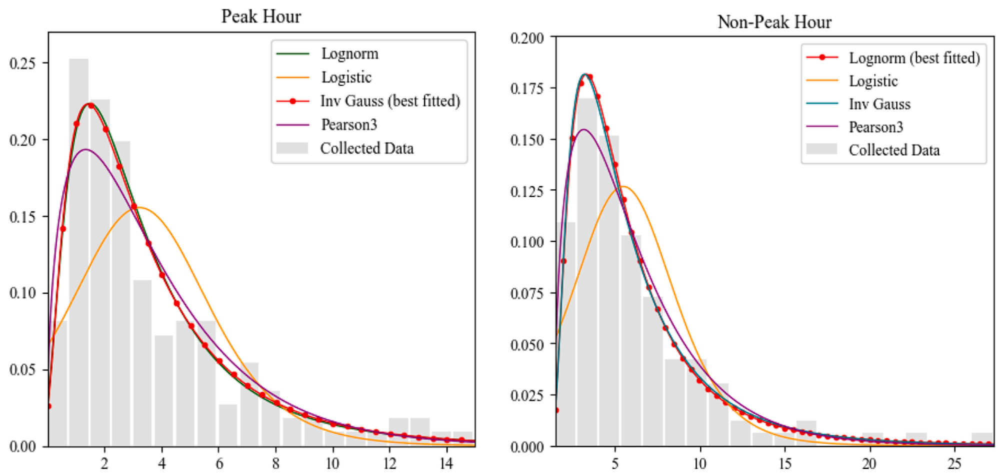

Fig. 9. Headway distribution fitting results

Table 4
Fitting errors of the headway distribution functions and parameter values

Period	distributions	Parameters μ	σ	SumSquare error	Best fit
Peak Hour	Lognormal	0.7205	-0.4215	0.0066	Inverse Gauss
	Loglogistic	3.2313	1.6089	0.0444	
	Inverse Gauss	0.5508	-0.6304	0.0065	
	Pearson 3	1.5936	3.7200	0.0147	
Non-Peak Hour	Lognormal	0.7286	0.9999	0.0005	Lognormal
	Loglogistic	5.4898	1.9761	0.0104	
	Inverse Gauss	0.5768	0.7587	0.0005	
	Pearson 3	1.5874	6.1198	0.0014	

trajectory is applicable for AVs. In the used simulation scenarios, the AV conducts a consecutive lane-changing on a three-lane freeway, and the AV's initial speed is 50 km/h or 80 km/h Fig. 10. displays the simulation results Fig. 10. (a) and (b) are the trajectory tracking and lateral acceleration results for the speed = 50 km/h, and Fig. 10 (c) and (d) are the results for the speed = 80 km/h. From Fig. 10, it can be concluded that the AV can successfully track the consecutive lane-changing trajectories planned by the third-order polynomial of Eq. (23).

Table 5
Model validation results

Period	Experimental section	ESP calculated by the model	ESP in the experiments	MAPE
Peak hour	A_1B_2	21.18%	19.93%	6.27%
	B_1C_1	69.58%	74.85%	7.04%
	C_3B_3	51.03%	58.33%	12.52%
	B_4A_2	37.87%	42.85%	11.62%
Non-Peak hour	A_1B_2	34.09%	31.44%	8.42%
	B_1C_1	72.57%	78.93%	8.06%
	C_3B_3	66.27%	59.21%	11.92%
	B_4A_2	52.06%	46.76%	11.34%

Table 6
Variables description in OpenACC

Variables	Descriptions
Time	Common time frame for all vehicles (s)
Speed	Raw Speed (Doppler) (m/s)
Lat	Latitude (rad)
Lon	Longitude (rad)
Alt	Altitude (m)
E	East (x) coordinate in the local ENU plane (common center for all vehicles) (m)
N	North (y) coordinate in the local ENU plane (common center for all vehicles) (m)
U	Up (z) coordinate in the local ENU plane (common center for all vehicles) (m)
IVS	Inter Vehicle Spacing computed from GNSS data after bumper to bumper correction (m)
Driver	The driver of the vehicle: manual driving or ACC driving

Table 7
Gipps' car-following model calibration and validation results

Calibration results of model parameters	Validation results
Reaction time = 0.2 s	Speed MAPE = 4.52%
Maximum acceleration = 3.0023 m/s^2	Position MAPE = 1.93%
Comfortable deceleration = -2.6298 m/s^2	
Minimum gap = 1.0058 m	
Desired deceleration of proceeding vehicle = -4.9966 m/s^2	

5. Simulation experiments and numerical analysis

In this section, the setup of the simulations is introduced first, and a simulation example is presented to explain the advantage of the proposed model. Following that, the influences of the several critical factors on ESP are analyzed by simulations. Furthermore, the variations of the OED point with the changes of the four factors, the initial lane, speed difference, average traffic speed, and weight value ω are explored by simulations.

5.1. Simulation setup

A simulation platform constructed using Python is used to perform simulation experiments. On the platform, the traffic flow is generated based on the headway distribution data collected in Section 4 and the fitted distribution function. A five-lane freeway is set up, and the average speeds of the vehicles on the five lanes are 55 km/h, 70 km/h, 85 km/h, 100 km/h, and 115 km/h respectively, as shown in Fig. 11. An AV on Lane 5 tends to leave the freeway, so Lane 5 is the initial decision lane (abbreviated as IDL in the paper). In Fig. 11, the red vehicle is the AV, and the blue, yellow, and red lines respectively represent the car-following state (CF), the gap-searching state (SS), and the lane-changing execution state (SE) of the AV. This simulation setup is set as the basic simulation scenario for the following simulations.

Based on the above simulation setup, the position of the OED point is obtained according to the proposed OED model, which is 4.5 km away from the off-ramp. From this point, the AV can meet 274 gaps, and ESP is 0.9746. To make a comparison, the simulations for the other two cases, the decision point is before the OED point, and the decision point is after the OED point, are conducted. Define the case that the AV makes a freeway-exiting decision just at the OED point (4.5 km) as Case 1, and define the cases that the decision point before and after the OED point as Case 2 and Case 3. The key variables can be obtained through the simulation platform, based on which the schematic freeway-exiting processes of the three cases are displayed in Fig. 12. It can be observed that the AV cannot reach Lane 1 before the off-ramp and fails to exit the freeway in Case 3, while the AV succeeds in Case 1 and Case 2, because the AV has too short a distance to reach the off-ramp in Case 3. Moreover, the AV merges onto Lane 1 at 162 s and exits the freeway at 235 s in Case 2. In comparison, the AV merges onto Lane 1 at 184 s and exits the freeway at 209 s in Case 1. The results indicate that the OED point

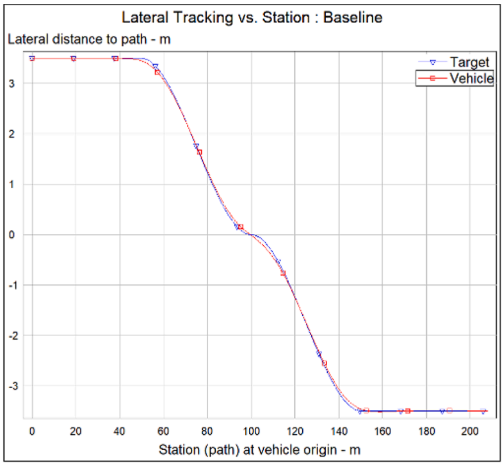

(a) Lane-changing trajectory with speed = 50 km/h

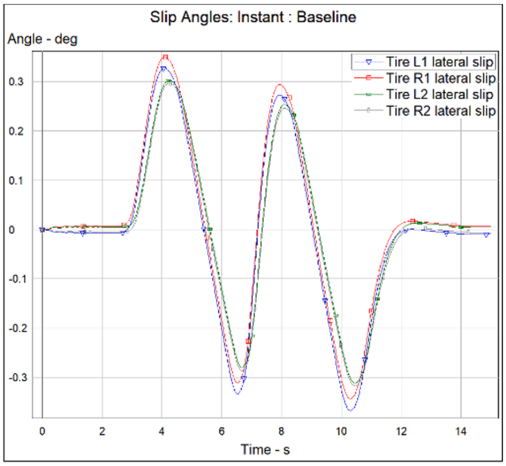

(b) Lateral acceleration with speed = 50 km/h

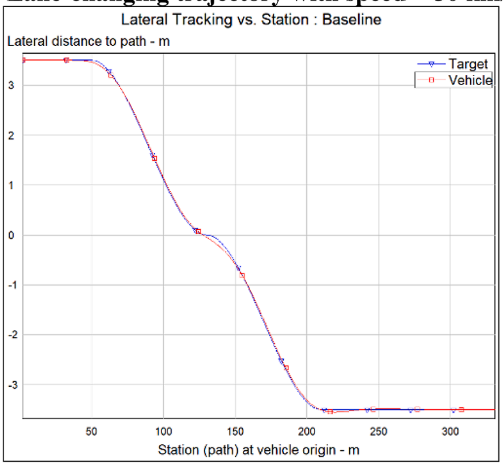

(c) Lane-changing trajectory with speed = 50 km/h

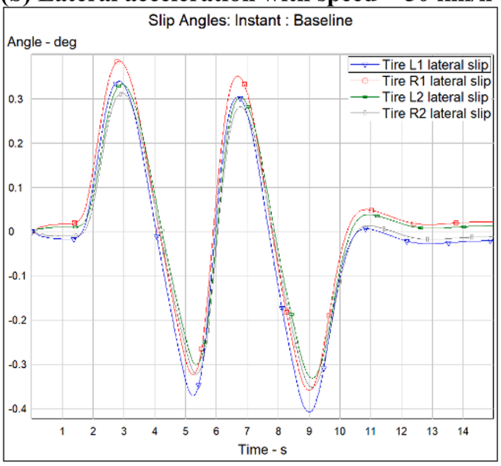

(d) Lateral acceleration with speed = 50 km/h

Fig. 10. Simulation results with CarSim

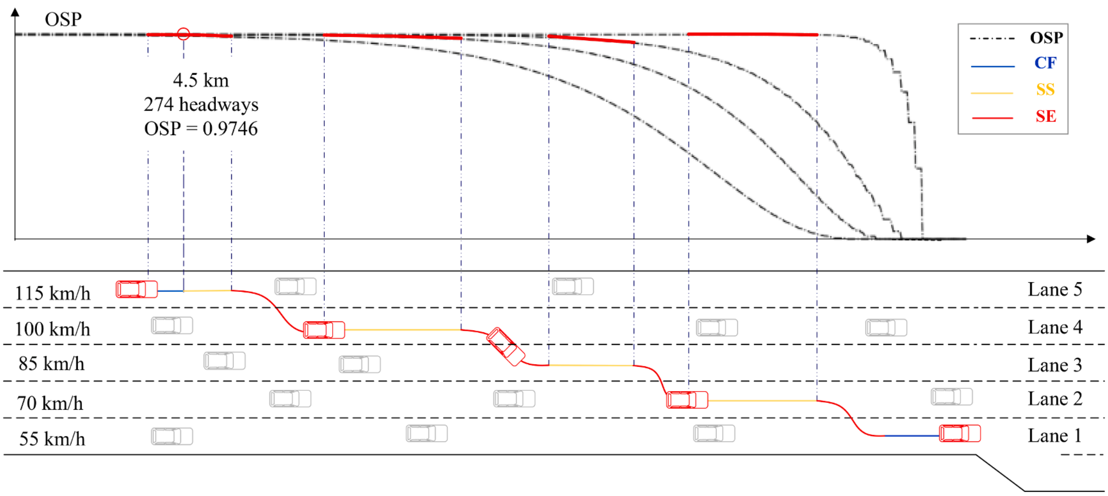

Fig. 11. Scenario used in the simulations

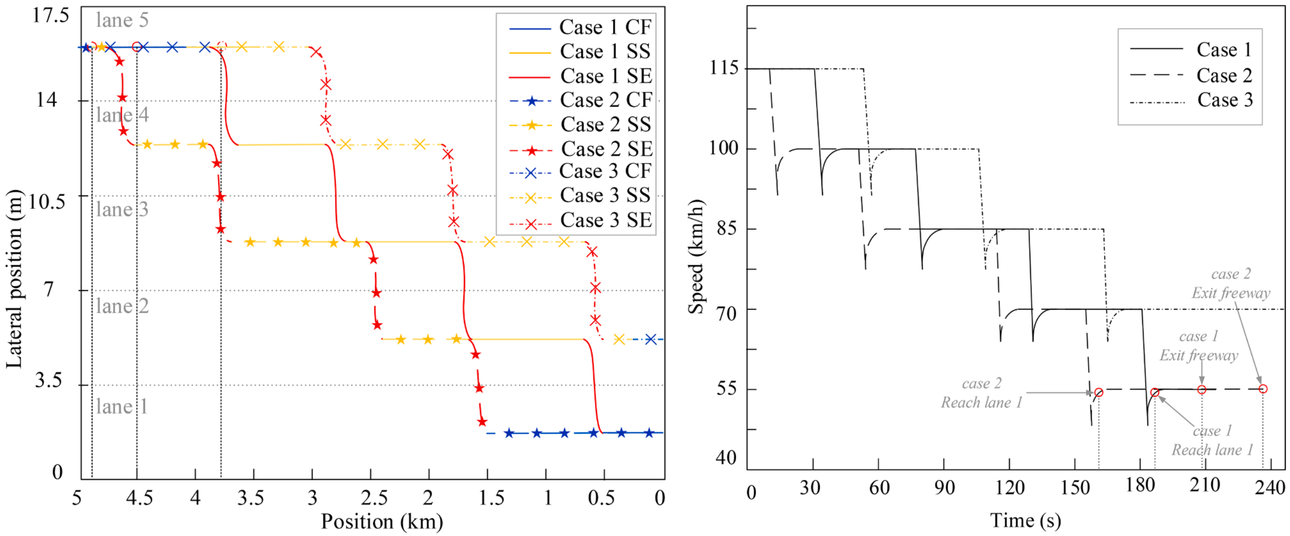

***(a)* Lateral position of the AV** ***(b)* Speed of the AV**

Fig. 12. Comparison of the three cases for different freeway-exiting decision positions

generated by the proposed model can help the AV leave the freeway successfully with high efficiency.

5.2. ESP analysis

The impacts of several key variables, including the initial decision lane, the speed difference between the two adjacent lanes, average traffic speed, and speed of the AV, on ESP are investigated. The simulation setup in 5.1 is used.

5.2.1. Initial decision lane

The AV is initially located on which lane when it first makes a freeway-exiting decision will significantly influence the following freeway-exiting process, so this point is explored here Fig. 13. displays the relationship between ESP and the freeway-exiting decision position for different IDLs. In the case that IDL is Lane 2, the position of the LLP is 178 m, and ESP is 0 when the decision position is less than 178 m. The positions of LLP are 224 m, 382 m, and 526 m for the cases of IDL = 3, 4, and 5, respectively. Thus, the LLP moves upstream with the increment of the number of IDL, which is consistent with the intuition. Moreover, it can be observed that the value of ESP increases gradually with the increment of the distance from the decision point to LLP, because the AV can meet more safe lane-changing gaps. For the same decision position, the value of ESP gradually decreases with the increment of the number of IDL, because the AV needs to across more lanes to reach the rightmost lane. In addition, when the value of ESP is higher than 0.9, it is assumed that the AV can successfully exit the freeway, so then the AV needs to start the freeway-exiting maneuver before 312 m, 1641 m, 2350 m, and 3227 m for the cases of IDL = 2, 3, 4, and 5 respectively.

5.2.2. Speed difference between the two adjacent lanes

Fig. 14 displays the variation of ESP with the changes of the distance from the decision point to the off-ramp (denoted as "Pos" in the figure) and the speed difference between the two adjacent lanes (Δv). In the simulations, the speed of vehicles on Lane 1 is set as 55 km/h, and Δv is increased gradually from 5 km/h to 23 km/h.

From Fig. 14, it can be observed that, with the increment of Δv, the value of ESP increases gradually until reaching its maximum value and then starts to decline gradually. For example, on the position of 1 km, ESP reaches its maximum value when $\Delta v = 11$ km/h, and on the position of 3 km, the maximum value of ESP appears when $\Delta v = 14$ km/h. The reason is that when Δv increases, the AV can meet more safe lane-changing gaps within a given period, which will increase the value of ESP. However, the increment of the Δv will also increase the average speed of the AV, which will reduce the time for the AV to find a safe lane-changing gap and further decrease the value of ESP. Therefore, the value of ESP can be increased by making Δv be in an appropriate range. However, this phenomenon is not obvious for the cases of Pos = 1 km and 6 km. The reason is that the value of ESP is always small due to the AV's short distance to the off-ramp in the case of 1 km, and the value of ESP is always large due to the AV's long distance from the decision point to the off-ramp in the case of 6 km, no matter what the value of Δv is.

5.2.3. Average speed of the traffic flow

The influence of the average speed of the traffic flow on ESP is simulated. Increase the average speed of the traffic flow from 45 km/h to 120 km/h gradually to observe the variation of ESP Fig. 15. displays the relationship between ESP and the decision position under different average speeds when IDL is Lane 4. From Fig. 15, it can be observed that the value of ESP increases with the increment of the distance from the exiting decision position to the off-ramp for a given average speed, which is consistent with the results of Subsection 5.2.1. The value of ESP decreases with the increment of the average speed at a given decision position. The reason is that as the average speed increases, the travel time from the decision point to the off-ramp decreases, so that the safe lane-changing gaps that the AV can meet decrease as well, resulting in the decrement of ESP. Thus, when the traffic speed is higher, the AV should start an exiting decision

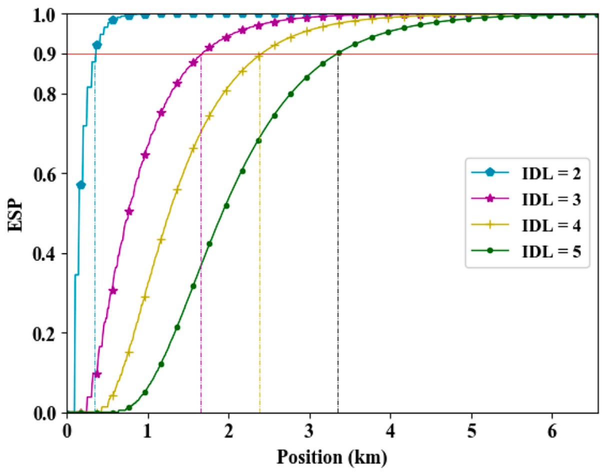

Fig. 13. Relationship between ESP and position with different IDLs

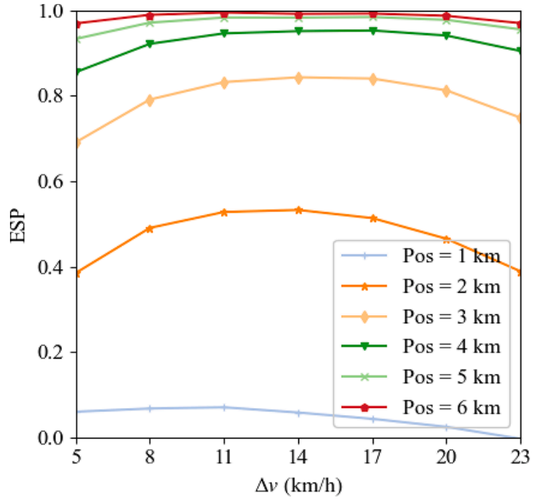

Fig. 14. ESP for different Δ*v* and decision positions

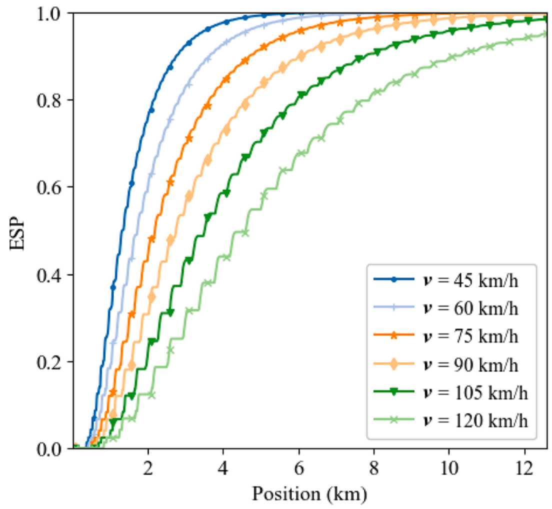

Fig. 15. Relationship between ESP and position with different average speeds

earlier to enhance the value of ESP.

Specifically, Fig. 16 illustrates the variations of ESP with the changes of the average speed for the two cases that the decision positions are 5 km and 2 km Fig. 16. (*a*) shows that the value of ESP decreases with the increase of traffic speed except for IDL = 2. When IDL = 2, the AV only needs to change one lane to exit the freeway, which is quite easy to achieve when the decision position is 5 km, so the average speed does not significantly impact ESP. In the other three cases, when the average speed increases, the time left for the AV to find an acceptable lane-changing gap is reduced, so the value of ESP decreases. In the case of IDL = 5, the value of ESP is high (more than 0.9) when the speed is below 70 km/h; however, it drops sharply as the average speed continues to increase. As a result, an alert should be sent to the AV in advance to prepare the AV once the average speed is higher than 70 km/h Fig. 16. (*b*) illustrated that the values of ESP are much smaller than those of decision positions at 5 km for the same IDL except for the case of IDL = 2. For the two cases of IDL = 4 and 5, a successful exiting for the AV cannot be ensured even when the average decreases to 45 km/h. Therefore, when the traffic speed is high, or IDL is far from the lane connecting to the off-ramp, the AV should initiate a freeway-exiting process earlier.

5.2.4. Speed of the AV

With the same starting point, the way AV performs the freeway-exiting also affects the ESP. Therefore, the influence of the AV's speed in the case of the two-lane scenario is investigated in this subsection. In the simulations, the IDL is Lane 2, and the decision position is taken as 2 km to the off-ramp. Keep the average speed of the vehicles on Lane 1 as 76 km/h, and change the speed of the AV from 40 km/h to 140 km/h gradually to observe the variation of ESP Fig. 17. illustrates that, with the increment of the speed of the AV, the value of ESP decreases when AV's speed is less than 76 km/h and increases when AV's speed is greater than 76 km/h (that is the

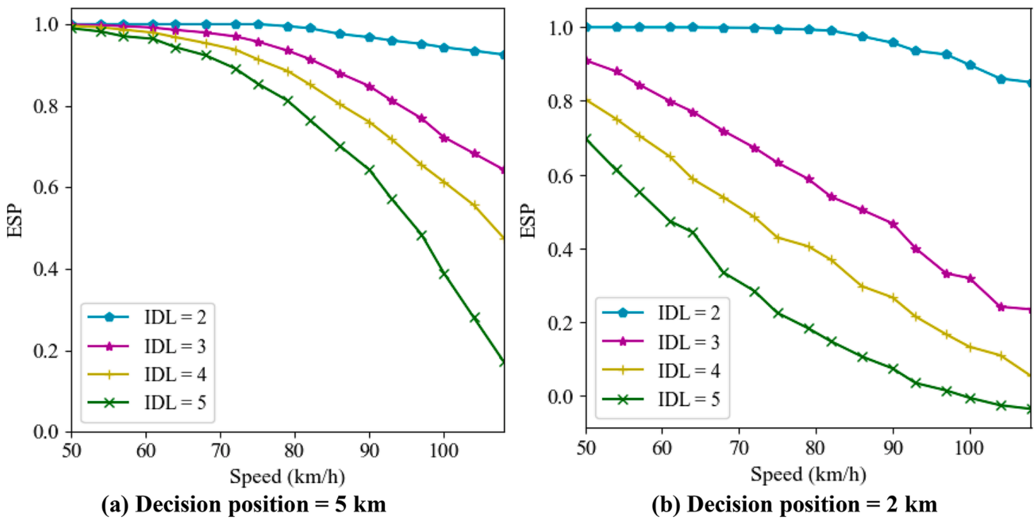

Fig. 16. Relationship between ESP and the average speed of the traffic flow

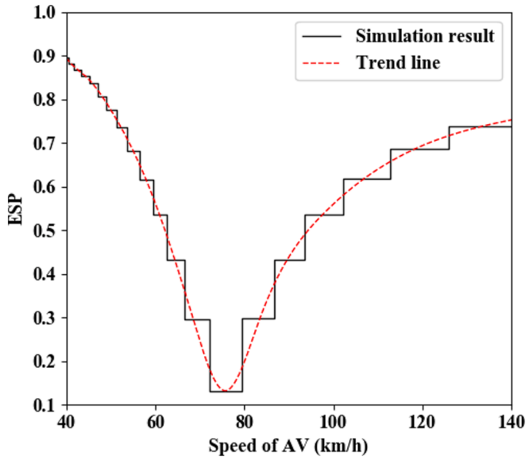

Fig. 17. Relationship between ESP and the speed of AV

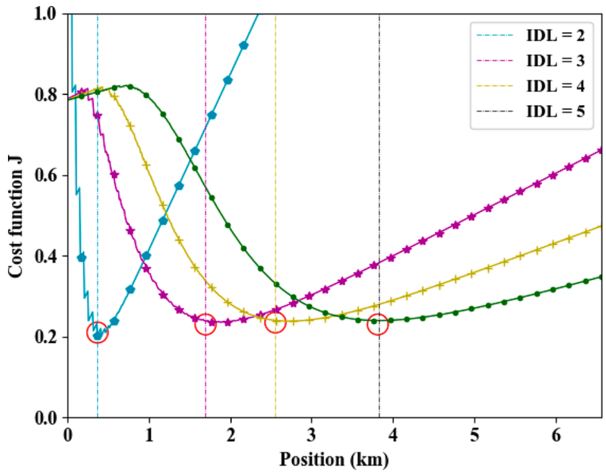

Fig. 18. Relationship between cost function J and the position of the OED point with different IDLs

average speed of vehicles on Lane 1). This phenomenon indicates that the ESP decreases with the decrement of the difference between the AV's speed and the average speed of the vehicles on the right lane. The reason is that when the speed difference between the AV and the average speed of the vehicles on the target lane decreases, the number of acceptable gaps that the AV can meet on the right lane in the remaining time will decrease as well. Therefore, both deceleration and acceleration can increase the value of ESP with the lowest ESP at around 76 km/h. Furthermore, the trendline is much steeper in the deceleration regime than in the acceleration regime. Such a phenomenon indicates that deceleration is more efficient in obtaining a high ESP. This may be because the deceleration is more likely to allow AV to match gaps on the target lane before reaching the off-ramp.

5.3. OED point analysis

5.3.1. Initial decision lane

In the simulations, the environment setup in Subsection 5.1 is still used, and the weight value ω is set as 0.3 Fig. 18. displays the variations of cost function J and the positions of the OED points for different IDLs in the cases of $\Delta v = 10$ km/h. From Fig. 18, it can be observed that the OED positions are 413 m, 1674 m, 2568 m, and 3896 m to the off-ramp, respectively, for the cases of the IDLs = 2, 3, 4, and 5. The position of the OED point moves upstream when the initial decision lane becomes further away from the lane connecting to the off-ramp, which is consistent with intuition. Moreover, comparing the positions corresponding to ESP = 0.9 in Fig. 13 and the OED points in Fig. 18, it can be found that the position corresponding to ESP = 0.9 may be before the OED point. In these cases, if still choosing OED point to initiate a freeway-exiting process, the AV may fail to leave the freeway. Thus, to ensure that the AV can successfully leave the freeway, a part of efficiency gains must be sacrificed. The position corresponding to ESP = 0.9 is chosen as the final exiting decision point.

5.3.2. Speed difference between the two adjacent lanes

This part explores how Δv between the two adjacent lanes influences the position of the OED point. In the simulations, the average speed of the vehicles on Lane 1 is set as 55 km/h, and Δv is increased from 3 km/h to 30 km/h gradually Fig. 19. (*a*) displays the relationship between the OED point position and Δv for the cases of IDL = 2, 3, 4, and 5. When IDL is Lane 3 or Lane 2, the position of the OED point decreases with the increment of Δv within the discussed range of Δv. When IDL is Lane 5 or Lane 4, the position of the OED point decreases with the increment of Δv until reaching its minimum value at some point and then starts to increase. The position of the OED point reaches its minimum value when Δv is15 km/h for the case of IDL = 5 and is 25 km/h for the case of IDL = 4. This phenomenon indicates an optimal Δv that can make the OED point closest to the off-ramp when IDL is Lane 5 or Lane 4. The reason is that the increment of Δv will increase the value of ESP, but the increment of the average speed will reduce the time for the AV to find a safe lane-changing gap Fig. 19. (*b*) displays the solution characteristics of Eq. (1) for $\Delta v = 9$ km/h, 15 km/h, and 21 km/h when IDL = 5. Simulations generate the results in the figure. In the figure, the three points are the solutions of Eq. (1), namely, the OED points of the three cases. Since the three cases have the same average speed on Lane 1, they have the same J'_1 curve. Compared to the case of $\Delta v = 9$ km/h, J'_2 is smaller in the case of $\Delta v = 15$ km/h, so the position of the OED point moves to the left from 4.4 km to 3.7 km. When Δv increases from 15 km/h to 21 km/h, the curve of J'_2 moves right and further causes that the distance from the OED point to the off-ramp to increase. Therefore, when the IDL is Lane 5, the position of the OED point in the case of $\Delta v = 15$ km/h is the smallest in the three cases.

5.3.3. Average speed of the traffic flow

The influence of the average speed of traffic flow on the OED point is investigated here. Maintain that Δv is 10 km/h, and increase

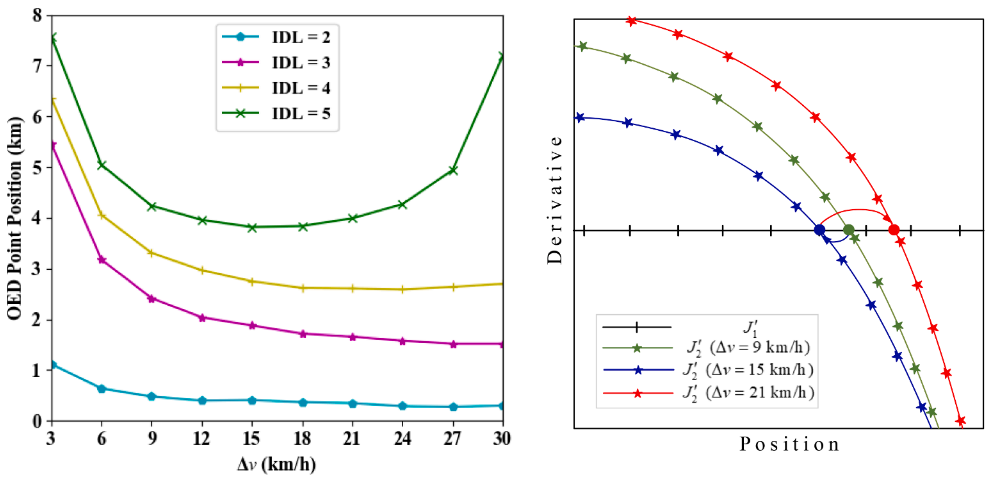

(*a*) Variation of the position of the OED point **(*b*) Process of solving the position of the OED point**

Fig. 19. Relationship between the position of the OED point and Δv with different IDLs

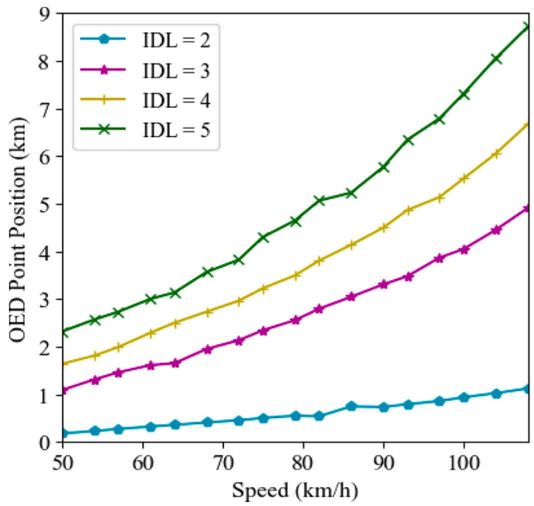

Fig. 20. Relationship between the OED point position and average speed with different IDLs

the average speed from 50 km/h to 120 km/h gradually Fig. 20. displays the variation of the OED point position with the change of the average speed when IDL = 2, 3, 4, and 5 Fig. 20. depicts that the distance from the OED point to the off-ramp increases when increasing the average speed at IDL = 3, 4, and 5. This result indicates that the OED point gradually moves upstream as the average speed increases, which means that the AV needs to initiate a freeway-exiting process earlier to leave the freeway when the traffic speed is higher. The reason is that the increment of the average speed will decrease the value of ESP, which further increases the distance from the OED point to the off-ramp. When IDL is Lane 2, the distance from the OED point to the off-ramp does not increase so significantly as in the other cases, and its value is always smaller than 1 km. For this case, the speed has a negligible effect on the OED point because the AV only needs to change one lane to exit the freeway, which is easy to be realized.

5.3.4. *Weight value ω for efficiency*

The influence of the weight value ω in the proposed OED model on the position of the OED point is investigated here. In the simulations, the average speed of the vehicles on Lane 1 is set as 55 km/h, and Δv is set as 10 km/h. Changing the weight value from 0.2 to 0.9 to observe the variation of the OED point Fig. 21. displays the relationship between the position of the OED point and ω for the cases of IDL = 2, 3, 4, and 5. In the figure, the position of the OED point decreases with the increment of ω, because that larger ω means more considerations of the driving efficiency in the decision, and the AV will tend to stay longer on the faster lanes. When IDL is 2, the AV can leave the freeway easily, so the position of the OED point does not change much and is relatively small. For the cases that IDL = 3, 4, and 5, the position of the OED point varies significantly with ω, and the slopes for the different cases are different. When the value of ω is between 0.45 and 0.65, the slope is the highest. When ω increases from 0.65 to 0.9, the change rate tends to be gentle, which happens because the value of ESP drops sharply when the AV gets too close to the ramp, neutralizing the effect of ω. With the

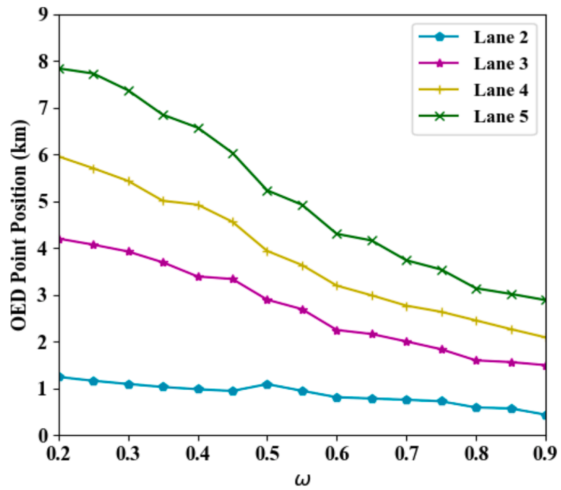

Fig. 21. Relationship between the position of the OED point and ω

decrement of ω in the range of [0.2, 0.45], the slopes decrease as well. The reason is that the value of ESP is quite high and approaching 1 in this case, and the AV does not need to sacrifice more efficiency to increase the success probability.

6. Conclusions and future work

This paper focuses on how an AV generates an appropriate freeway-exiting decision that can ensure the AV exit the freeway successfully with less travel time. An Exiting Success Probability (ESP) model for AVs is first proposed. Based on the ESP model, a new model to determine the optimal exiting decision (OED) point is developed. The proposed ESP model is validated using field data collected in Chengdu, China. Numerical simulations further analyze the characteristics of the proposed models. The following main conclusions are drawn in the paper.

(1) According to the validation results based on the field data, the MAPE of the proposed model is not more than 13%. The results indicate that the model can predict the freeway-exiting success probability with acceptable accuracy and can be applied to the AV to generate an appropriate freeway-exiting decision point in the freeway-exiting process.
(2) With the increment of the distance of the freeway-exiting decision position to LLP, the value of ESP increases and approaches 100% gradually. By evaluating ESP, the AV can choose an appropriate freeway-exiting decision position to ensure a high ESP but without sacrificing too much travel time in the freeway-exiting process.
(3) When the AV speed becomes closer to the average speed of the vehicles on the target lane, the value of the ESP of the AV decreases. An AV can enhance ESP by decreasing or increasing its speed to meet more safe lane-changing gaps on the target lane, and the speed-decreasing method has a more significant effect than the speed-increasing method.
(4) When the traffic speed is high on the freeway, the AV should start an exiting decision early to enhance the value of ESP. The value of the ESP can increase by making the speed difference between the two adjacent lanes be in an appropriate range.

The paper still has some limitations. First, the exiting decision problem of AVs is still explored in the traditional traffic environment, and how the connected vehicle technology impact the problem will be discussed in the future. Second, more experiments should be conducted to test the model reliability, which will be performed in the future.

Author statement

Manuscript title: Optimization Model for the freeway-exiting position decision problem of automated vehicles

I have made substantial contributions to the conception, design of the work; or the acquisition, analysis, or interpretation of data for the work; AND

I have drafted the work or revised it critically for important intellectual content; AND I have approved the final version to be published; AND

I agree to be accountable for all aspects of the work in ensuring that questions related to the accuracy or integrity of any part of the work are appropriately investigated and resolved.

All persons who have made substantial contributions to the work reported in the manuscript, including those who provided editing and writing assistance but who are not authors, are named in the Acknowledgments section of the manuscript and have given their written permission to be named. If the manuscript does not include Acknowledgments, it is because the authors have not received substantial contributions from nonauthors.

Acknowledgments

This work was National Natural Science Foundation of China (Grant No. 52172333), Fundamental Research Funds for the Central Universities (Grant No. 2682021ZTPY010), and Technical Research Plan of the Ministry of Public Security (2020JSYJA05).

References

Mobileye Starts Testing Self-Driving Vehicles in Germany [Online], 2020. Available. https://newsroom.intel.com/news/mobileye-starts-testing-self-driving-vehicles-germany/.
Ali, Y., Zheng, Z., Haque, M.M., Wang, M., 2019. A game theory-based approach for modelling mandatory lane-changing behaviour in a connected environment. Transp. Res. Part C 106, 220–242, 2019/09/01/.
Ardelt, M., Coester, C., Kaempchen, N., 2012. Highly automated driving on freeways in real traffic using a probabilistic framework. IEEE Trans. Intell. Transp. Syst. 13 (4), 1576–1585.
Awal, T., Murshed, M., Ali, M., 2015. An efficient cooperative lane-changing algorithm for sensor- and communication-enabled automated vehicles. In: 2015 IEEE Intelligent Vehicles Symposium (IV), pp. 1328–1333.
Berger, C., Rumpe, B., 2014. Autonomous driving-5 years after the urban challenge: the anticipatory vehicle as a cyber-physical system. arXiv preprint. *arXiv:1409.0413*.
Brockfeld, E., Kühne, R.D., Wagner, P., 2005. Calibration and Validation of Microscopic Models of Traffic Flow. Transp. Res. Rec. 1934 (1), 179–187, 2005/01/01.
Cao, P., Hu, Y., Miwa, T., Wakita, Y., Morikawa, T., Liu, X., 2017. An optimal mandatory lane change decision model for autonomous vehicles in urban arterials. J. Intell. Transp. Syst. 21 (4), 271–284, 2017/07/04.
Cui, H., et al., 2018. Multimodal trajectory predictions for autonomous driving using deep convolutional networks. arXiv preprint. *arXiv:1809.10732*.
Datta, T., Schattler, K.L., Guha, A., Kar, P., 2004. Development and evaluation of an advanced dynamic lane merge traffic control system for 3 To 2 lane transition areas in work zones. (in English), Tech Report.

Dong, C., Wang, H., Li, Y., Wang, W., Zhang, Z., 2020. Route control strategies for autonomous vehicles exiting to Off-Ramps. IEEE Trans. Intell. Transp. Syst. 21 (7), 3104–3116.

Dou, Y., Fang, Y., Hu, C., Zheng, R., Yan, F., 2018. Gated branch neural network for mandatory lane changing suggestion at the on-ramps of highway. IET Intel. Transport Syst. 13 (1), 48–54.

Gipps, P.G., 1986. A model for the structure of lane-changing decisions. Transp. Res. Part B 20 (5), 403–414, 1986/10/01/.

Gong, S., Du, L., 2016. Optimal location of advance warning for mandatory lane change near a two-lane highway off-ramp. Transp. Res. Part B 84, 1–30.

Greenberg, I., 1966. The log normal distribution of headways. Australian Road Research 2 (7), 8–14.

Hao, W., Zhang, Z., Gao, Z., Yi, K., Liu, L., Wang, J., 2020. Research on mandatory lane-changing behavior in highway weaving sections. J. Adv. Transp. 2020, 3754062, 2020/07/23.

Hart, P., Rychly, L., Knoll, A., 2019. Lane-merging using policy-based reinforcement learning and post-optimization. In: IEEE Intelligent Transportation Systems Conference (ITSC), pp. 3176–3181.

He, J., He, Z., Fan, B., Chen, Y., 2020. Optimal location of lane-changing warning point in a two-lane road considering different traffic flows. Physica A 540, 123000, 2020/02/15/.

Hou, Y., Edara, P., Sun, C., 2014. Modeling mandatory lane changing using bayes classifier and decision trees. IEEE Trans. Intell. Transp. Syst. 15 (2), 647–655.

Hu, X., Sun, J., 2019. Trajectory optimization of connected and autonomous vehicles at a multilane freeway merging area. Transp. Res. Part C 101, 111–125, 2019/04/01/.

Krizhevsky, A., Sutskever, I., Hinton, G.E., 2017. ImageNet classification with deep convolutional neural networks. Commun. ACM 60 (6), 84–90.

Kumar, A.V.S.S.B., Modh, A., Babu, M., Gopalakrishnan, B., Krishna, K.M., 2018. A novel lane merging framework with probabilistic risk based lane selection using time scaled collision cone. In: *IEEE Intelligent Vehicles Symposium (IV)*, Changshu, Suzhou, China.

Leclercq, L., Laval, J.A., Chiabaut, N., 2011. Capacity drops at merges: AN endogenous model. Transp. Res. Part B 45 (9), 1302–1313, 2011/11/01/.

Li, L., Li, X., 2019. Parsimonious trajectory design of connected automated traffic. Transp. Res. Part B 119, 1–21, 2019/01/01/.

Luo, Q., Saigal, R., Chen, Z., Yin, Y., 2019/11/01. Accelerating the adoption of automated vehicles by subsidies: a dynamic games approach. Transp. Res. Part B 129, 226–243. /2019.

Ma, J., Li, X., Zhou, F., Hu, J., Park, B.B., 2017. Parsimonious shooting heuristic for trajectory design of connected automated traffic part II: computational issues and optimization. Transp. Res. Part B 95, 421–441.

Mai, T., Jiang, R., Chung, E., 2016. A Cooperative Intelligent Transport Systems (C-ITS)-based lane-changing advisory for weaving sections. J. Adv. Transp. 50 (5), 752–768, 2016/08/01.

Makridis, M., Mattas, K., Anesiadou, A., Ciuffo, B., 2021. OpenACC. An open database of car-following experiments to study the properties of commercial ACC systems. Transp. Res. Part C 125, 103047, 2021/04/01/.

Mattioli, M., 2018. Autonomy in the age of autonomous vehicles. Boston Univ. J. Sci. Technol. Law 24, 101–125, 2018/6/27.

Maurya, A.K., Das, S., Dey, S., Nama, S., 2016. Study on speed and time-headway distributions on two-lane bidirectional road in heterogeneous traffic condition. Transp. Res. Procedia 17, 428–437, 2016/01/01/.

McCoy, P.T., Pesti, G., 2001. Dynamic Late Merge–Control Concept for Work Zones on Rural Interstate Highways. Transp. Res. Rec. 1745 (1), 20–26.

Nourinejad, M., Bahrami, S., Roorda, M.J., 2018. Designing parking facilities for autonomous vehicles. Transp. Res. Part B 109, 110–127.

Park, H., Smith, B.L., 2012. Investigating benefits of intellidrive in freeway operations: Lane changing advisory case study. J. Transp. Eng. 138 (9), 1113–1122.

Punzo, V., Simonelli, F., 2005. Analysis and comparison of microscopic traffic flow models with real traffic microscopic data. Transp. Res. Rec. 1934 (1), 53–63, 2005/01/01.

Saad, M., Abdel-Aty, M., Lee, J., Wang, L., 2018. Safety analysis of access zone design for managed toll lanes on freeways. J. Transp. Eng., Part A 144 (11), 04018067.

Schakel, W.J., Arem, B.v., 2014. Improving Traffic Flow Efficiency by In-Car Advice on Lane, Speed, and Headway. IEEE Trans. Intell. Transp. Syst. 15 (4), 1597–1606.

Shladover, S.E., 2018. Connected and automated vehicle systems: Introduction and overview. J. Intell. Transp. Syst. 22 (3), 190–200.

Singh, S., Kumar, A., Niyas, M., Santhakumar, M., 2020. Multivariate analysis of freeways speed and time headway under mixed traffic streams. In: 2020 International Conference on COMmunication Systems & NETworkS (COMSNETS), pp. 116–121.

Sun, D., Benekohal, R.F., 2005. Analysis of work zone gaps and rear-end collision probability. J. Transp. Stat. 8 (2), 71–86.

Sun, J., Zheng, Z., Sun, J., 2020. The relationship between car following string instability and traffic oscillations in finite-sized platoons and its use in easing congestion via connected and automated vehicles with IDM based controller. Transp. Res. Part B 142, 58–83, 2020/12/01/.

Tarko, A.P., Shamo, D., Wasson, J., 1999. Indiana lane merge system for work zones on rural freeways. J. Transp. Eng. 125 (5), 415–420.

Vechione, M., Balal, E., Cheu, R.L., 2018. Comparisons of mandatory and discretionary lane changing behavior on freeways. Int. J. Transp. Sci. Technol. 7 (2), 124–136, 2018/06/01/.

Wu, J., Hu, J., Sun, J., 2010. Departure headway distribution modeling for ordinary large cities based on video information. In: 5th International Conference on Computer Sciences and Convergence Information Technology, pp. 1040–1045.

Yang, D., Zheng, S., Wen, C., Jin, P.J., Ran, B., 2018. A dynamic lane-changing trajectory planning model for automated vehicles. Transp. Res. Part C 95, 228–247, 2018/10/01/.

Yang, D., Zhou, Q., Shen, Y., Xiong, M., Xu, L., 2020. A human-like lane-changing trajectory planning model for automated vehicles based on an improved safety-sensitive LSTM-NN Model. In: presented at the Transportation Research Board Annual Meeting.

Yang, M., Wang, X., Quddus, M., 2019. Examining lane change gap acceptance, duration and impact using naturalistic driving data. Transp. Res. Part C 104, 317–331, 2019/07/01/.

Yang, Q.I., Koutsopoulos, H.N., 1996. A Microscopic Traffic Simulator for evaluation of dynamic traffic management systems. Transp. Res. Part C 4 (3), 113–129, 1996/06/01/.

Yu, C., Sun, W., Liu, H.X., Yang, X., 2019. Managing connected and automated vehicles at isolated intersections: From reservation- to optimization-based methods. Transp. Res. Part B 122, 416–435, 2019/04/01/.

Yuan, J., Abdel-Aty, M., Cai, Q., Lee, J., 2019. Investigating drivers' mandatory lane change behavior on the weaving section of freeway with managed lanes: a driving simulator study. Transp. Res. Part F 62, 11–32, 2019/04/01/.

Zhang, C., Sabar, N.R., Chung, E., Bhaskar, A., Guo, X., 2019. Optimisation of lane-changing advisory at the motorway lane drop bottleneck. Transp. Res. Part C 106, 303–316, 2019/09/01/.

Zhang, L., Chen, C., Zhang, J., Fang, S., You, J., Guo, J., 2018. Modeling lane-changing behavior in freeway off-ramp areas from the shanghai naturalistic driving study. J. Adv. Transp. 2018, 8645709, 2018/01/14.

Zhou, Y., Ahn, S., 2019. Robust local and string stability for a decentralized car following control strategy for connected automated vehicles. Transp. Res. Part B 125, 175–196, 2019/07/01/.

Zhou, Y., Ahn, S., Wang, M., Hoogendoorn, S., 2020/02/01. Stabilizing mixed vehicular platoons with connected automated vehicles: an H-infinity approach. Transp. Res. Part B 132, 152–170. /2020.